JOURNAL OF FINANCIAL AND QUANTITATIVE ANALYSIS Vol. 60, No. 7, Nov. 2025, pp. 3551–3590
© THE AUTHOR(S), 2025. PUBLISHED BY CAMBRIDGE UNIVERSITY PRESS ON BEHALF OF THE MICHAEL G. FOSTER SCHOOL OF BUSINESS, UNIVERSITY OF WASHINGTON
doi:10.1017/S0022109025000079

The New Keynesian Model and Bond Yields

Martin M. Andreasen
Aarhus University and Danish Finance Institute
mandreasen@econ.au.dk

Abstract

This article presents a New Keynesian model to capture the linkages between macro fundamentals and the nominal yield curve. The model explains bond yields with a low level of news in expected inflation and plausible term premia. This implies that the slope of the yield curve predicts future bond yields and that risk-adjusted historical bond yields satisfy the expectations hypothesis. The model also explains the spanning puzzle, matches key moments for real bond yields, captures the evolution of the price-dividend ratio, and implies that the slope of the yield curve and the price-dividend ratio forecast excess equity returns.

I. Introduction

The New Keynesian model is one of the most prominent models in macroeconomics to understand the dynamics of economic activity, inflation, and the monetary policy rate. The model has also implications for prices on financial assets, although these prices often are ignored. The market for nominal government bonds is of particular interest because bond yields contain information about expected future policy rates and term premia, where the latter is determined by consumption and inflation risk. However, it is well known that the model struggles to explain bond yields, mainly because term premia are too low and too stable (see, e.g., Rudebusch and Swanson (2008)). This is obviously a concern because prices are the key device that ensure equilibrium in the model, as emphasized by Cochrane (2007).

Much work has, therefore, been devoted to improve the New Keynesian model along this dimension.[1] The inclusion of recursive preferences by Rudebusch and Swanson (2012) is crucial in this context because these preferences allow an otherwise standard New Keynesian model to generate plausible term premia without distorting macro fundamentals. In this model, news about expected inflation is a key driver of bond yields. However, Duffee (2018) shows that this implication is not consistent with data for the United States (U.S.), and this finding, therefore, challenges the current specification of bond yields and inflation dynamics in the New Keynesian model.

This article modifies the New Keynesian model to explain macro fundamentals *and* bond yields with a low level of news in expected inflation. The proposed

I thank Robert Goldstein (the referee), Kasper Jørgensen, Anders Bredahl Kock, Dennis Kristensen, Giovanni Pellegrino, Morten Ravn, and Daniel Wilhelm for useful comments and discussions. I also appreciate comments from participants at the Cemmap seminar at the University College London.

[1]See, for instance, Hordahl, Tristani, and Vestin (2008), Graeve, Emiris, and Wouters (2009), Bekaert, Cho, and Moreno (2010), Dew-Becker (2014), Kung (2015), Bretscher, Hsu, and Tamoni (2020), and Meyer-Gohde and Kliem (2022), among others.

https://doi.org/10.1017/S0022109025000079 Published online by Cambridge University Press

https://doi.org/10.1017/S0022109025000079 Published online by Cambridge University Press

model generates realistic term premia that have the same level and variability as in reduced-form dynamic term structure models (DTSMs). In addition, the model satisfies the two requirements in Dai and Singleton (2002) for a correct specification of term premia, which serve as useful diagnostic tests given that term premia are unobserved. The first requirement is that the difference between long- and short-term bond yields (i.e., the yield spread) predicts future bond yields as in Campbell and Shiller (1991). This property of bond yields is evaluated using a long simulated sample and is, therefore, an unconditional test of term premia. The second requirement is that historical bond yields satisfy the expectations hypothesis once adjusted for term premia using the proposed model. This second requirement is, therefore, a conditional test of term premia, in the sense that it requires reliable state and term premia estimates for historical bond yields. We also show that the nonlinear structure of the model generates variation in key macro variables that is not explained in linear regressions of these macro variables on bond yields. That is, the model *endogenously* produces unspanned variation in macro variables as observed in U.S. data, and it, therefore, goes a long way in avoiding the critique of macro-finance term structure models raised in Joslin, Priebsch and Singleton (2014). The model also provides a close fit to real bond yields, although they are not included when estimating the model. Taking the analysis beyond bond yields, we finally show that the model captures the overall evolution in the price-dividend ratio and that excess equity returns are predictable based on the yield spread and the price-dividend ratio, as documented by Fama and French (1989). Here, and throughout we restrict relative risk aversion to 10, meaning that we do not rely on extreme levels of risk aversion to explain asset prices from macro fundamentals.

Two features of our model are essential to obtain these results. First, we use the flexible formulation of recursive preferences in Andreasen and Jørgensen (2020) to separate the intertemporal elasticity of substitution (IES), the relative risk aversion (RRA), *and* the timing attitude. In contrast, the standard formulation of recursive preferences only separates the IES and the RRA, while the timing attitude follows directly from the IES and RRA. With this flexible formulation of recursive preferences, demand shocks is found to be a key driver of bond yields, their embedded term premia, and key macro variables, but not of inflation. This is different from the standard formulation of recursive preferences, where bond yields and term premia are mainly determined by productivity shocks, as shown in Rudebusch and Swanson (2012). However, productivity shocks have a sizable effect on inflation and hence explain bond yield dynamics with too much variation in expected inflation, as emphasized by Duffee (2018).

Second, the New Keynesian model is typically solved using a third-order perturbation approximation because it allows for time-varying term premia unlike the standard log-linear approximation widely used in macroeconomics. The perturbation approximation and its risk adjustment for the variables of interest $\mathbf{y}_t$ are obtained at the deterministic steady state $\mathbf{y}_{ss}$, but the approximation is applied around the unconditional mean $\mathbb{E}[\mathbf{y}_t]$. This extrapolation typically works well when $\mathbf{y}_{ss}$ is reasonably close to $\mathbb{E}[\mathbf{y}_t]$. However, we generally find that this difference is large with recursive preferences estimated to match U.S. bond yields and that this leads to poor performance of the perturbation approximation, even when considering expansions up to fifth order. We address this previously unnoticed

shortcoming of the perturbation approximation by instead using the projection method of Judd (1992), which is computed on a grid around $\mathbb{E}[\mathbf{y}_t]$. To greatly improve its computational efficiency, we note that for a given stochastic discount factor the solution to all bond prices is given in closed form by ordinary least squares (OLS) and hence obtained instantaneously. The same holds for expected future short rates and hence for term premia. These closed form solutions represent a new methodological contribution to the projection literature and apply to many popular choices of basis functions and to any approximation order. We show that the estimates for several parameters in the New Keynesian model change substantially when using the projection approximation instead of the less accurate but widely used third-order perturbation approximation.

The remainder of this article is organized as follows: Section II presents the New Keynesian model, while our estimation approach is described in Section III. The main empirical results are provided in Section IV, with various sensitivity results provided in Section V. Additional model implications are discussed in Section VI, and Section VII concludes.

II. A New Keynesian Model

A. The Households

We consider an infinitely lived representative household with recursive preferences as in Epstein and Zin (1989) and Weil (1990). Using the formulation in Rudebusch and Swanson (2012), the value function V_t is given by

$$V_t = u_t + \beta\left(\mathbb{E}_t\left[V_{t+1}^{1-\alpha}\right]\right)^{1/(1-\alpha)}, \tag{1}$$

when the utility function $u_t > 0$ for all t.[2] The subjective discount factor $\beta \in (0,1)$ and $\mathbb{E}_t[\cdot]$ denotes the conditional expectation in period t. The main purpose of $\alpha \in \mathbb{R}\setminus\{1\}$ is to endow the household with preferences for when uncertainty is resolved, unless $\alpha = 0$ and equation (1) reduces to expected utility. It follows from Kreps and Porteus (1978) that equation (1) implies preferences for early (late) resolution of uncertainty if $\alpha > 0$ ($\alpha < 0$) for $u_t > 0$, whereas the opposite sign restrictions apply when $u_t < 0$. Andreasen and Jørgensen (2020) further argue that the size of this timing attitude is proportional to α, meaning that numerically larger values of α generate stronger preferences for early (late) resolution of uncertainty.

The utility function $u_t \equiv u(c_t, l_t)$ is assumed to depend on the number of consumption units c_t bought in the goods market and the provided labor supply l_t to firms. Following Andreasen and Jørgensen (2020), we also include a constant u_0 in the utility function to account for utility from goods and services that are not acquired in the goods market. This could be utility from government spending or utility from goods produced and consumed within the household. As shown in Andreasen and Jørgensen (2020), the reason for introducing u_0 is to separately control the level of the utility function to disentangle the timing attitude α from relative risk aversion (RRA), which otherwise are tightly linked in the standard

[2] When $u_t < 0$, $V_t = u_t - \beta\mathbb{E}_t\left[\left(-V_{t+1}\right)^{1-\alpha}\right]^{\frac{1}{1-\alpha}}$ as in Rudebusch and Swanson (2012).

https://doi.org/10.1017/S0022109025000079 Published online by Cambridge University Press

formulation of recursive preferences. Using a power specification to quantify the utility from market consumption c_t and similarly for leisure $1-l_t$, we let

$$u(c_t,l_t)=\frac{d_t}{1-\chi}(c_t-bc_{t-1})^{1-\chi}+z_t^{1-\chi}\left(d_t n_t\varphi_0\frac{(1-l_t)^{1-\frac{1}{\varphi}}}{1-\frac{1}{\varphi}}+u_0\right). \tag{2}$$

The parameter $b\geq 0$ accommodates external consumption habits, which are included to capture autocorrelation in consumption growth. The variable d_t introduces shocks to the utility function to temporally increase or decrease the utility from a given level of c_t and l_t, implying that d_t operates as a demand shock.[3] The variable n_t is also exogenous and temporally shifts the household's incentive between c_t and l_t, meaning that n_t may be interpreted as a labor supply shock. Market consumption grows with the rate of the productivity level z_t, and it is therefore necessary to scale the utility from leisure and nonmarket consumption by $z_t^{1-\chi}$ to ensure that these terms do not diminish relative to $\frac{1}{1-\chi}(c_t-bc_{t-1})^{1-\chi}$ along the balanced growth path. This scaling is discussed and motivated further in Rudebusch and Swanson (2012) and Andreasen and Jørgensen (2020).

The parameter $\chi>0$ and the degree of habit formation b determine the steady state intertemporal elasticity of substitution (IES) as $\left(1-b\mu_{z,ss}^{-1}\right)/\chi$, which measures the percentage change in market consumption growth for a 1-percent change in the real interest rate when ignoring uncertainty. The endogenous labor supply gives the household an additional margin to absorb shocks and this modifies existing expressions for RRA. Using the results in Swanson (2018), it follows that RRA in the steady state is

$$\mathrm{RRA}=\frac{\chi}{\left(1-\frac{b}{\mu_{z,ss}}\right)+\chi\varphi\frac{\tilde{w}_{ss}^*(1-l_{ss})}{\tilde{c}_{ss}}}+\frac{\alpha(1-\chi)}{(1-\chi)u_0\tilde{c}_{ss}^{\chi-1}\left(1-\frac{b}{\mu_{z,ss}}\right)^{\chi}+\left(1-\frac{b}{\mu_{z,ss}}\right)+\frac{1-\chi}{1-\frac{1}{\varphi}}\frac{\tilde{w}_{ss}^*(1-l_{ss})}{\tilde{c}_{ss}}},$$

where $\tilde{c}_{ss}=c_t/z_t\big|_{ss}$ and $\tilde{w}_{ss}^*=w_t^*/z_t\big|_{ss}$ refer to the steady state (ss) of market consumption and the real frictionless wage w_t^* relative to the productivity level, with $\mu_{z,ss}$ being the steady state growth rate of the productivity level. Given that the IES is determined by χ, and α controls the strength of the timing attitude, the level of the utility function u_0 is the key parameter for determining RRA.

The real budget constraint is $c_t+\mathbb{E}_t\left[M_{t,t+1}x_{t+1}^{real}\right]=x_t^{real}/\pi_t+w_t^*l_t+Div_t+T_t$. That is, resources are spent on market consumption goods c_t and nominal state-contingent claims X_{t+1}, where $x_{t+1}^{real}\equiv X_{t+1}/P_t$ denotes the real value of these claims

[3] In the endowment models of Albuquerque, Eichenbaum, Luo, and Rebelo (2016) and Gomez-Cram and Yaron (2021), shocks to the utility function affect only asset prices and are therefore referred to as capturing valuation risk. In production-based equilibrium models, shocks to d_t generate also endogenous variation in consumption, inflation, etc., and this explains why these shocks are referred to as demand shocks within these models.

https://doi.org/10.1017/S0022109025000079 Published online by Cambridge University Press

that are priced using the nominal stochastic discount factor $M_{t,t+1}$. The household's income is given by the real value of state-contingent claims bought in the previous period x_t^{real}/π_t, the real wage income $w_t^* l_t$, real dividend payments from firms Div_t, and real lump-sum transfers T_t. Here, π_t denotes the gross inflation rate.

The first-order conditions for the utility maximizing household are

$$\mathbb{E}_t[M_{t,t+1}R_t] = 1 \tag{3}$$

$$z_t^{1-\chi} n_t \varphi_0 (1-l_t)^{-\frac{1}{\varphi}} = (c_t - bc_{t-1})^{-\chi} w_t^*, \tag{4}$$

where R_t is gross 1-period nominal interest rate. Equation (3) is the well-known consumption Euler-equation, while equation (4) is the optimality condition for the labor supply.

To incorporate wage stickiness, we follow Blanchard and Gali (2005), Rudebusch and Swanson (2008), among others and introduce a simple wage bargaining friction in the labor market. Specifically, we assume that the real market wage w_t is given by

$$w_t = \kappa_w(\tilde{w}_{ss} z_t) + (1-\kappa_w) w_t^*, \tag{5}$$

where $\kappa_w \in [0,1)$ captures wage stickiness by smoothing the frictionless wage w_t^* in relation to the long-term wage along the balanced growth path $\tilde{w}_{ss} z_t$. Although this simple wage rule does not explicitly introduce Nash bargaining between workers and firms, Blanchard and Gali (2005) argue that it is a parsimonious way to capture the essential features of real wage bargaining.

B. The Firms

Output y_t is produced by a competitive representative firm, which combines differentiated intermediate goods $y_t(i)$ using $y_t = \left(\int_0^1 y_t(i)^{\frac{\eta-1}{\eta}} di\right)^{\frac{\eta}{\eta-1}}$ with $\eta > 1$. The demand for the ith good is given by $y_t(i) = \left(\frac{P_t(i)}{P_t}\right)^{-\eta} y_t$, where $P_t \equiv \left(\int_0^1 P_t(i)^{1-\eta} di\right)^{\frac{1}{1-\eta}}$ denotes the aggregate price level and $P_t(i)$ is the price of the ith good.

Intermediate firms produce slightly differentiated goods using the production function $y_t(i) = z_t a_t k_{ss}^{\theta} l_t(i)^{1-\theta}$, where k_{ss} and $l_t(i)$ denote capital and labor services at the ith firm, respectively. The variables a_t and z_t capture transitory and permanent productivity shocks, respectively. Each intermediate firm can freely adjust its labor demand at the given market wage w_t. Price stickiness is introduced as in Rotemberg (1982), where $\xi \geq 0$ controls the size of firms' real cost $\frac{\xi}{2}(P_t(i)/(P_{t-1}(i)\pi_{ss}) - 1)^2 y_t$ when changing $P_t(i)$. As in Rudebusch and Swanson (2012), each firm uses $\delta k_{ss} z_t$ units of output for investment to maintain a constant capital stock along the balanced growth path. The first-order conditions for profit maximization are

$$w_t = mc_t(1-\theta) z_t a_t k_{ss}^{\theta} l_t^{-\theta} \tag{6}$$

https://doi.org/10.1017/S0022109025000079 Published online by Cambridge University Press

$$(7)\quad y_t(1-\eta)+\mathbb{E}_t\left[\xi M_{t,t+1}\pi_{t+1}\left(\frac{\pi_{t+1}}{\pi_{ss}}-1\right)\frac{\pi_{t+1}}{\pi_{ss}}y_{t+1}\right]+mc_t y_t\eta=\xi\left(\frac{\pi_t}{\pi_{ss}}-1\right)y_t\frac{\pi_t}{\pi_{ss}},$$

where mc_t denotes marginal costs. Equation (6) determines labor demand, and equation (7) implies an aggregate supply relation between output and inflation.

The aggregate resource constraint reads $c_t+z_t\delta k_{ss}=\left(1-\frac{\xi}{2}\left(\frac{\pi_t}{\pi_{ss}}-1\right)^2\right)y_t$, where $\frac{\xi}{2}\left(\frac{\pi_t}{\pi_{ss}}-1\right)^2 y_t$ is the output loss from price stickiness.[4]

C. The Central Bank

The policy rate for the Federal Reserve is the short (1-period) nominal rate R_t. It is set according to the forward-looking Taylor-rule

$$(8)\qquad R_t=R_{ss}\mathbb{E}_t\left[\exp\left\{\phi_\pi\log\left(\frac{\pi_{t+1}}{\pi_{ss}\pi^*_{t+1}}\right)+\phi_{\Delta c}(\Delta c_{t+1}-\Delta c_{ss})\right\}\right],$$

based on a desire to stabilize future inflation π_{t+1} and future economic activity as measured by consumption growth Δc_{t+1}. To accommodate the large variation in inflation in postwar U.S. data, we follow the existing literature and introduce an exogenous inflation target π^*_t around the steady state inflation rate π_{ss}.

D. Bond Pricing and Structural Shocks

The price in period t of a default-free zero-coupon bond $B^{(k)}_t$ maturing in k periods with a face value of \$1 is $B^{(k)}_t=\mathbb{E}_t\left[M_{t,t+1}B^{(k-1)}_{t+1}\right]$ for $k=1,\ldots,n_b$ with $B^{(0)}_t=1$. Using continuos compounding, the yield to maturity is $r^{(k)}_t=-\frac{1}{k}b^{(k)}_t$ with $b^{(k)}_t\equiv\log B^{(k)}_t$. Bond prices are, therefore, determined by the nominal stochastic discount factor, which reads

$$(9)\qquad M_{t,t+1}=\beta\frac{d_{t+1}}{d_t}\left(\frac{c_{t+1}-bc_t}{c_t-bc_{t-1}}\right)^{-\chi}\left(\frac{\left(\mathbb{E}_t\left[V^{1-\alpha}_{t+1}\right]\right)^{\frac{1}{1-\alpha}}}{V_{t+1}}\right)^{\alpha}\frac{1}{\pi_{t+1}}$$

when $u_t>0$ for all t. The term premium $TP^{(k)}_t$ is defined as the difference between $r^{(k)}_t$ and the expected future path of the short rate, i.e., $TP^{(k)}_t=r^{(k)}_t-\sum_{i=0}^{k-1}\mathbb{E}_t[r_{t+i}]$ with $r_t\equiv\log R_t$.

Finally, we use a standard specification for the five structural shocks by letting

[4]Here we abstract from any costs linked to wage stickiness by setting the household transfers $T_t=l_tw_t-l_tw^*_t=\kappa_w l_t\left((\tilde{w}_{ss}z_t)-w^*_t\right)$ to ensure that the wage bill w_tl_t paid by the firms is also the wage bill received by the household.

https://doi.org/10.1017/S0022109025000079 Published online by Cambridge University Press

$$
\begin{aligned}
\log(\mu_{z,t+1}/\mu_{z,ss}) &= \rho_{\mu_z}\log(\mu_{z,t}/\mu_{z,ss}) + \sigma_{\mu_z}\varepsilon_{\mu_z,t+1} \\
\log d_{t+1} &= \rho_d \log d_t + \sigma_d \varepsilon_{d,t+1} \\
\log n_{t+1} &= \rho_n \log n_t + \sigma_n \varepsilon_{n,t+1} \\
\log \pi^*_{t+1} &= \rho_{\pi^*}\log \pi^*_t + \sigma_{\pi^*}\varepsilon_{\pi^*,t+1} \\
\log a_{t+1} &= \rho_a \log a_t + \sigma_a \varepsilon_{a,t+1}
\end{aligned} \tag{10}
$$

with $\mu_{z,t} \equiv z_t/z_{t-1}$, where $\epsilon_{\mu_z,t+1}$, $\epsilon_{d,t+1}$, $\epsilon_{n,t+1}$, $\epsilon_{\pi^*,t+1}$, and $\epsilon_{a,t+1}$ are standard normally distributed and independent across time, denoted $\mathcal{NID}(0,1)$, and mutually uncorrelated.

III. Estimation Methodology

This section outlines how we estimate the New Keynesian model. We describe the considered data in Section III.A and present our solution method in Section III.B. The adopted estimation routine is discussed in Section III.C.

A. Data

The model is estimated using quarterly U.S. data from 1961:Q2 to 2019:Q3, where we end the sample before the start of the COVID-19 pandemic. The dynamics of the macro economy is measured by i) detrended labor supply $\widehat{l}_t$, ii) the detrended real wage $\widehat{w}_t$, iii) consumption growth Δc_t, and iv) inflation π_t.[5] The nominal yield curve is represented by the 3-month, 1-, 3-, 5-, 7-, and 10-year bond yields. These yields are taken from Gürkaynak, Sack, and Wright (2007), except at the 3-month maturity where we use the implied rate on a 3-month Treasury Bill.

Taylor-rules such as the one considered in equation (8) are obviously an approximation to the historical policy decisions taken by the Federal Reserve. In particular, the rule ignores the "monetarist experiment" from 1979:Q4 to 1982:Q4 and the policy rate being constrained by the 0 lower bound (ZLB) after 2008. We account for both of these deviations from the adopted interest rule in the following way.

First, during the monetarist experiment, the Federal Reserve targeted monetary aggregates and its policy decisions were, therefore, not well summarized by the interest rule in equation (8). To avoid that the highly volatile short rate in this period distorts the estimation, we greatly downweight the importance of the 3-month interest rate from 1979:Q4 to 1982:Q4 in the estimation. As explained in Section III.C, the model is estimated using nonlinear filtering techniques, and we implement this downweighting by increasing the standard deviation of the measurement errors for the 3-month interest rate to 100 basis points from 1979:Q4 to 1982:Q4.

[5]The labor supply is measured by the total number of employees for total nonfarm payrolls, while the real wage is measured by the seasonally adjusted real hourly compensation in the nonfarm business sector. Both variables are detrended using the procedure in Hamilton (2018). The consumption growth rate is calculated from real per capita nondurables and service expenditures. Inflation is measured by the year-on-year growth rate in the consumer price index (CPI) excluding food and energy prices for all urban consumers.

https://doi.org/10.1017/S0022109025000079 Published online by Cambridge University Press

https://doi.org/10.1017/S0022109025000079 Published online by Cambridge University Press

Second, the interest rule in equation (8) does not enforce the ZLB. A possible concern is therefore that the model may generate a short rate during the estimation that is clearly below 0 although the empirical short rate is always positive. We guard against this possibility by lowering the standard deviation of the measurement in the 3-month rate to just 5 basis points at the ZLB. This also ensures that the signal-to-noise ratio for the 3-month rate remains reasonable at the ZLB, where the variability in the short rate is greatly reduced. We define the ZLB as spells where the 3-month interest rate is below 50 basis points.

In total, the estimation uses 10 variables, which we collect in the vector $\mathbf{y}_t^{obs}$ and express in annualized terms except for $\widehat{l}_t$ and $\widehat{w}_t$.

B. Model Solution

The state variables for the model appear in the vector $\mathbf{x}_t = \left[\log\left(\frac{c_{t-1}}{z_{t-1}}\right) \log\mu_{z,t} \ \log d_t \ \log n_t \ \ \log\pi_t^* \ \ \log a_t\right]'$, where consumption is scaled by the productivity level z_t to ensure stationarity. All the remaining variables appear in the vector $\mathbf{y}_t$ with dimensions $n_y \times 1$. The exact solution is

$$\begin{aligned} \mathbf{y}_t &= \mathbf{g}(\mathbf{x}_t;\boldsymbol{\theta}) \\ \mathbf{x}_{t+1} &= \mathbf{h}(\mathbf{x}_t;\boldsymbol{\theta}) + \eta\boldsymbol{\epsilon}_{t+1} \end{aligned} \tag{11}$$

with $\boldsymbol{\epsilon}_t = \left[\epsilon_{\mu_z,t} \ \epsilon_{d,t} \ \epsilon_{n,t} \ \epsilon_{\pi^*,t} \ \epsilon_{a,t}\right]'$ and all structural coefficients collected in $\boldsymbol{\theta}$. The law of motions for the exogenous states are provided in equation (10), and the dynamics of $\log\left(\frac{c_{t-1}}{z_{t-1}}\right)$ is identical to the one for consumption scaled by z_t in $\mathbf{g}(\mathbf{x}_t;\boldsymbol{\theta})$. As a result, we only need to approximate the **g**-function.

The solution to the New Keynesian model with asset prices is typically obtained using a third-order perturbation approximation, because it allows for non-zero and time-varying risk premia. Although this approximation is often found to be very accurate as shown in Aruoba, Fernandez-Villaverde, and Rubio-Ramirez (2006) and Caldara, Fernandez-Villaverde, Rubio-Ramirez, and Yao (2012), the inclusion of recursive preferences generates a large risk adjustment that may reduce the accuracy of the approximation. The reason is that the risk adjustment to capture term premia in the perturbation approximation is computed around the deterministic steady state of $\mathbf{y}_t$, denoted $\mathbf{y}_{ss}$, but applied around the unconditional mean of $\mathbf{y}_t$, denoted $\mathbb{E}[\mathbf{y}_t]$. This extrapolation typically works well when $\mathbf{y}_{ss}$ is reasonably close to $\mathbb{E}[\mathbf{y}_t]$. However, we generally find that this difference is large with recursive preferences estimated to match U.S. bond yields, and this leads to poor performance of the perturbation approximation. For instance, in our baseline specification of the New Keynesian model, the annualized short rate has a determinist steady state of 18.50% but an unconditional mean of just 4.80%.[6]

Based on this observation, we instead solve the model by the projection method of Judd (1992) using a second-order polynomial for the **g**-function. Feasibility obviously dictates this relative low approximation order with $n_x = 6$ states,

[6]The main problem appears to be that the perturbation method struggles to accurately approximate V_t and $\mathbb{E}_t\left[V_{t+1}^{1-\alpha}\right]$, which then spills over into large approximations errors for bond yields.

$n_y = 45$ control variables, and $n_\varepsilon = 5$ structural shocks in the model. Nevertheless, as we show in Section V.B, the global nature of this solution provides a more accurate approximation when compared to even a fifth-order perturbation solution, in part because the risk correction in the projection approximation is computed on a grid around $\mathbb{E}[\mathbf{y}_t]$ and not around $\mathbf{y}_{ss}$. That is, we let

$$\mathbf{y}_t = \mathbf{g}_0 + \mathbf{g}_{\mathbf{x}}\mathbf{x}_t + \mathbf{g}_{\mathbf{xx}} vech\left(\mathbf{x}_t \mathbf{x}_t'\right), \tag{12}$$

where the unknown loadings for this projection approximation appear in $\mathbf{g}_0$, $\mathbf{g}_{\mathbf{x}}$, and $\mathbf{g}_{\mathbf{xx}}$ with dimensions $n_y \times 1$, $n_y \times n_x$, and $n_y \times n_x(n_x+1)/2$, respectively. We consider N grid points $\mathcal{X} = \{\mathbf{x}_i\}_{i=1}^N$ for the states and determine these unknown loadings by minimizing the model's Euler-equation errors on this grid. Details on the construction of the grid $\mathcal{X}$, evaluation of the conditional expectations in the Euler-equations, and the construction of the objective function are standard and provided in Appendix A.

For an efficient implementation, consider the partition $\mathbf{y}_t = \left[\left(\mathbf{y}_t^a\right)' \left(\mathbf{y}_t^b\right)' \left(\mathbf{b}_t^{zc}\right)' \right]'$, where $\mathbf{y}_t^a = \left[\log\left(\frac{c_t}{z_t}\right) \log \pi_t \log evf_t \right]'$ contains the three macro variables required to solve the model without any bond yields, with $evf_t = \mathbb{E}_t\left[\left(V_t / z_t^{1-\chi} \right)^{1-\alpha} \right]$ being an auxiliary variable used to capture the recursive preferences. The vector $\mathbf{y}_t^b = \left[\log l_t \log\left(\frac{w_t}{z_t}\right) \right]'$ represents additional macro variables used in the estimation, while all log-transformed zero-coupon bond prices appear in $\mathbf{b}_t^{zc} = \left[b_t^{(1)} \;\; b_t^{(2)} \;\; \dots \;\; b_t^{(40)} \right]'$. As shown in Appendix A, only the optimization step with respect to the unknown loadings related to $\mathbf{y}_t^a$ is nonlinear. Given the solution for $\mathbf{y}_t^a$, the projection loadings for $\mathbf{y}_t^b$ and $\mathbf{b}_t^{zc}$ are given in closed form by OLS and hence obtained instantaneously. We also show that the same holds for expected future short rates and hence for term premia. These closed form solutions for bond prices $\mathbf{b}_t^{zc}$ and expected short rates represent a new methodological contribution to the projection literature for models with a yield curve and extends to other basis functions than the one applied in equation (12) and to any approximation order. As a result, we are able to obtain a second-order projection approximation in just about 6 seconds on a standard desktop computer using a single CPU.[7] Exploiting this new computational trick is absolutely essential for making a formal estimation of our medium-sized New Keynesian model computational feasible with a global solution routine.

C. Robustified Inference with Nonlinear Filtering

The approximated state space representation of the model includes nonlinear terms with the unobserved states $\mathbf{x}_t$, implying that the Kalman filter cannot be used

[7]The processor is an AMD Ryzen 7 PRO 7840U. We reserve the use of multi-processing for the estimation of the structural parameters using the evolutionary optimization routine of Andreasen (2010) applied to the objective function described in Section III.C.

https://doi.org/10.1017/S0022109025000079 Published online by Cambridge University Press

to estimate the model. Instead, we rely on the central difference Kalman filter (CDKF) developed by Norgaard, Poulsen, and Ravn (2000), which is a nonlinear extension of the Kalman filter. The CDKF accommodates measurement errors in $\mathbf{y}_t^{obs}$, which in practice also include potential modelling errors. We specify these errors $\mathbf{v}_t$ to be uncorrelated Gaussian white noise, as typically assumed when estimating structural macroeconomic models and reduced-form DTSMs. That is, $\mathbf{v}_t \sim \mathcal{NID}(\mathbf{0}, \mathbf{R}_\mathbf{v})$ where $\mathbf{R}_\mathbf{v}$ is a diagonal covariance matrix, implying that $\mathbf{y}_t^{obs} = \mathbf{S}\mathbf{y}_t + \mathbf{v}_t$ for an appropriate selection matrix $\mathbf{S}$.[8]

A likelihood function can be derived from the CDKF under the assumption that the prediction errors for $\mathbf{y}_t^{obs}$ are Gaussian. However, this distributional specification does not hold exactly due to the nonlinear terms in the model solution. The CDKF, therefore, only provides a quasi log-likelihood function $\frac{1}{T}\sum_{t=1}^{T}\mathcal{L}_t(\boldsymbol{\theta})$, which can be used for a quasi maximum likelihood (QML) estimation, as suggested in Andreasen (2013).

A possible limitation of any QML approach (as with standard maximum likelihood) is its lack of robustness to model misspecifications other than the distributional assumption of the prediction errors for $\mathbf{y}_t^{obs}$. A possible source of misspecification in the New Keynesian model is that the same structural parameters in $\boldsymbol{\theta}$ determine the **g**- and the **h**-function. In contrast, the widely used reduced-form Gaussian DTSM basically allows these two functions to be determined by separate parameters, which in these models is essential to generate term premia dynamics that are not rejected by historical data (see Dai and Singleton (2002)).[9] In the context of the New Keynesian model, the **g**-function is likely to prefer large and persistent shocks, because this helps the model to generate variation in term premia and hence fit medium- and long-term bond yields. On the other hand, small and less persistent shocks are typically needed in the **h**-function to fit the state dynamics and ensure sensible unconditional properties of $\mathbf{y}_t^{obs}$. Given the inclusion of several bond yields with small measurement errors in the estimation, our experience is that the **g**-function dominates the QML estimates of the New Keynesian model. This typically implies a tight in-sample fit to $\mathbf{y}_t^{obs}$, but it comes at the expense of unconditional variances for $\mathbf{y}_t^{obs}$ that are too large compared to U.S. data.

Thus, a robustified version of the standard QML estimator is required to obtain reliable estimates of our New Keynesian model. The solution we propose is to shrink the QML estimator to the unconditional first and second moments of $\mathbf{y}_t^{obs}$ because this is a simple and transparent way to increase the weight assigned to the **h**-function in the estimation. We denote the shrinkage moments by $\frac{1}{T}\sum_{t=1}^{T}\mathbf{m}_t$ in the sample and by $\mathbb{E}[\mathbf{m}(\boldsymbol{\theta})]$ in the model. The applied estimator is given by

[8]Unlike the more accurate particle filter proposed in Fernández-Villaverde and Rubio-Ramírez (2007), the updating rule for the states in the CDKF is linear, implying that the recursive filtering equations only depend on first and second moments. The CDKF approximates these moments by a deterministic sampling procedure, and this makes the CDKF computationally much faster than any particle filter and generally also more accurate than the well-known extended Kalman filter.

[9]The only link between the **g**- and **h**-functions in the reduced-form Gaussian DTSM is the conditional covariance matrix of the states, but the effect of this covariance matrix on the **g**-function is typically very small.

https://doi.org/10.1017/S0022109025000079 Published online by Cambridge University Press

$$\hat{\boldsymbol{\theta}} = \arg\max_{\boldsymbol{\theta}\in\Theta} \frac{1}{T}\sum_{t=1}^{T}\mathcal{L}_t(\boldsymbol{\theta}) - \lambda \mathbf{f}_{1:T}(\boldsymbol{\theta})'\mathbf{W}\mathbf{f}_{1:T}(\boldsymbol{\theta}), \tag{13}$$

where Θ is the feasible domain of $\boldsymbol{\theta}$, $\mathbf{f}_{1:T}(\boldsymbol{\theta}) \equiv \frac{1}{T}\sum_{t=1}^{T}\mathbf{f}_t(\boldsymbol{\theta})$ with $\mathbf{f}_t(\boldsymbol{\theta}) \equiv \mathbf{m}_t - \mathbb{E}[\mathbf{m}(\boldsymbol{\theta})]$, and $\mathbf{W}$ is a diagonal weighting matrix containing the inverse of the standard errors for the shrinkage moments.[10]

The nature of the estimator in equation (13) is determined by $\lambda \geq 0$, which controls the weight assigned to the shrinkage moments relative to the sample average of $\mathcal{L}_t(\boldsymbol{\theta})$. We obviously recover the standard QML estimator when $\lambda = 0$, while $\hat{\boldsymbol{\theta}}$ converges to the generalized method of moments (GMM) estimator of Hansen (1982) when λ becomes sufficiently large. We consider a small amount of shrinkage by letting $\lambda = T$, which in our setting implies that shrinkage constitutes a small part of the objective function. Our results are not particularly sensitive to increasing the degree of shrinkage further, although we do find notable effects of shrinkage when compared to the standard QML estimator.[11]

To obtain closed-form expressions for the model-implied shrinkage moments, we apply the pruning scheme of Andreasen, Fernandez-Villaverde, and Rubio-Ramirez (2018) when setting up the state space system for the approximated version of the model.[12] This implies that the estimator in equation (13) can be implemented without resorting to simulation and belongs to the general class of extremum estimators. Its asymptotic properties are, therefore, easily derived in the Supplementary Material.

We use two classes of shrinkage moments. The first class contains first and second unconditional moments of $\mathbf{y}_t^{obs}$, except for the mean of detrended labor supply and the real wage that are 0. These moments help to robustify the QML estimates, which we illustrate in a Monte Carlo study in the Supplementary Material. Here, we show that shrinkage toward these moments give smaller parameter biases than standard QML when the model is misspecified with the **g**- and **h**-functions determined by different structural parameters. On the other hand, without any model misspecification, we unexpectedly find no benefit of shrinkage, which mainly reduces the efficiency of the standard QML estimator that is nearly unbiased in this case. We benchmark these results to using an extreme degree of shrinkage

[10] Another possibility is to use the optimal weighting matrix, but this version of equation (13) is not considered to avoid well-known small-sample distortions from estimating large covariance matrices in moment-based estimators. In our application, we estimate the diagonal elements in $\mathbf{W}$ using the Newey-West estimator with 3 lags.

[11] Note also that equation (13) belongs to the class of Laplace type or quasi-Bayesian estimators of Chernozhukov and Hong (2003), where a potentially misspecified log-likelihood function (as considered in our case) may be used within a Bayesian setting. When this estimator is combined with the endogenours prior specification in Christiano, Trabandt, and Walentin (2011) using a pre-sample of length T^*, we obtain the objective function in equation (13) with $\lambda = T^*/2$, as shown in the Supplementary Material.

[12] The pruning scheme is not essential in our case, because the proposed model has only one endogenous state (i.e., $\log(c_{t-1}/z_{t-1})$), and partly for this reason appears to be stable when simulated without pruning. Details related to the pruned state space system and the derivations of its moments are provided in the Supplementary Material.

https://doi.org/10.1017/S0022109025000079 Published online by Cambridge University Press

https://doi.org/10.1017/S0022109025000079 Published online by Cambridge University Press

with $\lambda = 10^6$, which corresponds to estimating the structural parameters by GMM and obtaining the states afterward by the CDKF. The Monte Carlo study shows that these GMM estimates of $\boldsymbol{\theta}$ display notable biases in finite samples and are clearly less efficient compared to the standard QML estimator ($\lambda = 0$) and the proposed estimator (with $\lambda = T$), both with and without model misspecification. These imprecise GMM estimates of the structural parameters also imply less accurate state estimates when compared with the proposed estimator with $\lambda = T$.

The second class of moments we include contain information about term premia as captured by the regression of Campbell and Shiller (1991). That is,

$$r_{t+m}^{(k-m)} - r_t^{(k)} = \alpha_k + \beta_k \frac{m}{k-m}\left(r_t^{(k)} - r_t^{(m)}\right) + u_{t+m,k}, \tag{14}$$

where $u_{t+m,k}$ is an error term and $m = 4$ to obtain annual changes in bond yields for our quarterly sample. The expectations hypothesis implies $\beta_k = 1$, but empirical estimates of the slope coefficients β_k are negative and decreasing with maturity, which is evidence of time-varying term premia. This implies that bond returns are predictable because equation (14) is equivalent to the forecast regression $rx_{t+m}^{(k)} = \tilde{\alpha}_k + \tilde{\beta}_k\left(r_t^{(k)} - r_t^{(m)}\right) + \varepsilon_{t+m,k}$, where $rx_{t+m}^{(k)}$ is excess bond returns and $\tilde{\beta}_k \equiv \frac{m}{4}(1-\beta_k)$. We consider β_k at the 2-, 3-, …, 10-year maturity to assign more weight to the evidence against the expectations hypothesis than implied by the considered panel of bond yields used to compute the quasi log-likelihood function. These slope coefficients are represented in the shrinkage moments by including $Cov\left(r_{t+m}^{(k-m)} - r_t^{(k)}, r_t^{(k)} - r_t^{(m)}\right)$ and $Var\left(r_t^{(k)} - r_t^{(m)}\right)$ related to β_k at the included maturities.

IV. Estimation Results

This section presents the main results for the proposed model. We proceed by discussing the estimated parameters in Section IV.A and the model fit in Sections IV.B to IV.D. The following three subsections explore how well the model matches key moments of bond yields that are *not* included in the estimation. The key mechanisms in the model are finally explained in Section IV.H.

A. Estimated Parameters

Not all parameters in the New Keynesian model are well-identified from our set of observables, and these parameters are, therefore, determined by standard calibration arguments. Hence, we let $\delta = 0.025$, $l_{ss} = 0.33$, and $\theta = 0.4$ as typically assumed for the U.S. economy. We also set the ratio of capital to output in the steady state to 2.5, as in Rudebusch and Swanson (2012). The value of $\mu_{z,ss}$ is set to match the mean of consumption growth, implying that $\mu_{z,ss} = 1.0055$. Finally, we set the constant u_0 in the utility function to get a steady state RRA of 10, as considered in Bansal and Yaron (2004).

Given the large number of variables included in the estimation, we set the size of the measurement errors in $\mathbf{y}_t^{obs}$ using reasonable assumptions. The standard

deviation for the measurement errors in all bond yields is set to 25 basis points, corresponding to 8.3% of the average standard deviations in the six considered yields. Similarly, we assume that 20% of the variation in labor supply, the real wage, and consumption growth is due to measurement errors, implying standard deviations of 58, 44, and 35 basis points, respectively. Inflation displays very similar dynamics to short-term bond yields, and we therefore set its measurement errors to 10% of its variation, as it gives a standard deviation of 24 basis points.

The first column in Table 1 reports the estimated parameters in the preferred version of the model. This baseline model is denoted $\mathcal{M}^{M,CS}$, where the superscripts indicate that shrinkage is applied based on the considered first and second unconditional moments of $\mathbf{y}_t^{obs}$ (by "M") and the selected Campbell-Shiller moments (by "CS"). The results for the other versions of the model will be discussed in Section V. For our preferred model $\mathcal{M}^{M,CS}$, we find $\widehat{\beta} = 0.991$ and a moderate degree of habit formation with $\widehat{b} = 0.65$. For consumption growth, this implies autocorrelations of 0.65, 0.42, 0.27, and 0.17 at the first 4 lags, which are reasonably close to the responding sample moments of 0.47, 0.37, 0.39, and 0.18, respectively. For the curvature parameter in the utility function, we get $\widehat{\chi} = 5.83$, which together with our estimate of b imply an IES of 0.06. This relatively low IES is consistent with Hall (1988) and Yogo (2004), who estimate the IES to between 0 and 0.2.

The degree of substitutability among the intermediate goods is $\eta = 8.85$, giving a low and plausible average price markup of 13%. To aid the interpretation of the price adjustment parameter ξ, Table 1 reports the corresponding Calvo parameter $\widehat{\xi}_{Calvo}$ that gives the same slope of the aggregate supply relation as $\widehat{\xi}$ when linearizing this relation.[13] We find $\widehat{\xi}_{Calvo} = 0.44$, which corresponds to an average price duration of just 1.8 quarters, showing that our New Keynesian model does not impose a strong degree of price stickiness. Instead, the model relies more on real wage stickiness with $\widehat{\kappa}_w = 0.92$, which is similar to the finding in Smets and Wouters (2007).

In relation to the labor supply, we find $\widehat{\varphi} = 0.10$ and therefore a Frisch elasticity of $\varphi(1/l_{ss} - 1) = 0.20$ in the steady state with $l_{ss} = 0.33$. Most micro estimates of the Frisch labor supply elasticity for males are in the range from 0.10 to 0.40 according to Keane (2011), showing that our low estimate of ϕ is consistent with micro evidence. With $\widehat{\phi}$ and $\widehat{\chi}$ well below and above 1, respectively, the utility function in equation (2) is negative. Hence, the estimate $\widehat{\alpha} = -11.46$ implies preferences for early resolution of uncertainty and a realistic timing premium of 2.81%. As discussed in Epstein, Farhi, and Strzalecki (2014), this means that the household is willing to give up 2.81% of total lifetime consumption to have all uncertainty resolved in the following period. Given these estimates, we obtain the required relative risk aversion of 10 when the utility constant is $u_0 = -459$. To interpret the magnitude of this constant, we compute the periodic utility $u(c_t, l_t)$ with and without a constant in a simulated sample to find the fraction of utility from consumption and leisure, that is, $u(c_t, l_t)|_{u_0=0}/u(c_t, l_t)$. This fraction has an average of 12% but displays considerable variation over the business cycle with a 5th percentile of 3% and a 95th percentile of 26%. As a result, the constant u_0 ensures a high and, therefore, also more stable utility level relative to its mean when

[13] The mapping between ξ and ξ_{Calvo} is $\xi = \frac{(1-\theta+\eta\theta)(\eta-1)\xi_{Calvo}}{(1-\xi_{Calvo})(1-\theta)\left(1-\xi_{Calvo}\beta\mu_{z,ss}^{1-\chi}\right)}$.

https://doi.org/10.1017/S0022109025000079 Published online by Cambridge University Press

TABLE 1

The Structural Parameters

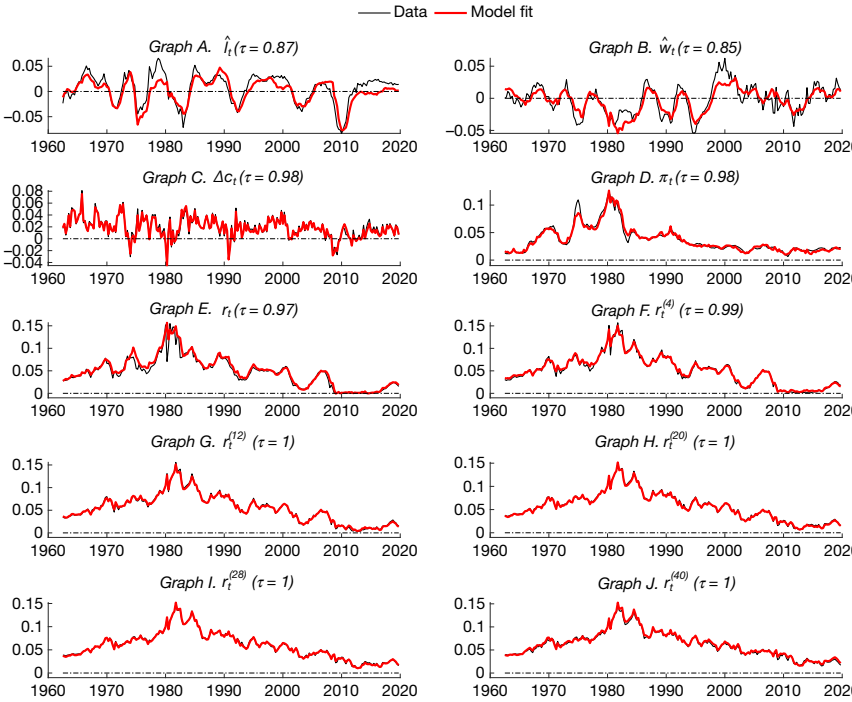
Table 1 shows the estimated parameters using quarterly data from 1961 to 2019, with asymptotic standard errors provided in parentheses. The first 4 observations are used to initialize the CDKF. The use of shrinkage is denoted on the model object by using the superscipts "M" for the unconditional moments and "CS" for the Campbell-Shiller moments. The subscript on the model object indicates that the standard specification of recursive preferences (EZ) is used in column 4 and that a third-order perturbation approximation (3rd) to the model solution is used in column 5. No standard errors are provided for β, η, and $\phi_{\Delta c}$ when they are at their upper bounds of 0.999, 10, and 10, respectively. The timing premium is evaluated at the steady state and computed as in Andreasen and Jørgensen (2020).

	$\mathcal{M}^{M,CS}$	$\mathcal{M}^{M}$	$\mathcal{M}$	$\mathcal{M}^{M,CS}_{EZ}$	$\mathcal{M}^{M,CS}_{3th}$
	1	2	3	4	5
α	–11.460	–9.029	–9.032	–16.488	–14.250
	(6.214)	(1.664)	(0.630)	(3.788)	(2.367)
β	0.991	0.999	0.988	0.993	0.948
	(0.011)	–	(0.000)	(0.003)	(0.057)
b	0.653	0.574	0.841	0.866	0.625
	(0.077)	(0.007)	(0.010)	(0.116)	(0.268)
φ	0.098	0.092	0.156	0.209	0.169
	(0.065)	(0.003)	(0.003)	(0.045)	(0.347)
χ	5.828	7.104	5.042	1.948	15.633
	(1.101)	(0.309)	(0.630)	(0.550)	(13.174)
ξ_{Calvo}	0.438	0.309	0.497	0.772	0.396
	(0.086)	(0.003)	(0.026)	(0.008)	(0.230)
κ_w	0.917	0.909	0.834	0.867	0.945
	(0.016)	(0.020)	(0.001)	(0.045)	(0.017)
η	8.848	10.000	10.000	8.208	9.774
	(11.414)	–	–	(2.166)	(0.763)
ϕ_π	3.957	3.691	4.764	2.982	10.000
	(2.321)	(0.880)	(1.558)	(0.830)	–
$\phi_{\Delta c}$	1.096	0.658	4.572	2.344	2.940
	(0.442)	(0.563)	(1.532)	(2.600)	(0.799)
ρ_{μ_z}	0.491	0.373	0.540	0.770	0.218
	(0.128)	(0.075)	(0.000)	(0.046)	(0.272)
ρ_d	0.984	0.985	0.968	0.978	0.998
	(0.001)	(0.000)	(0.005)	(0.002)	(0.010)
ρ_n	0.986	0.985	0.984	0.967	0.980
	(0.008)	(0.005)	(0.004)	(0.041)	(0.026)
ρ_{π^*}	0.995	0.989	0.985	0.997	0.987
	(0.011)	(0.000)	(0.009)	(0.003)	(0.015)
ρ_a	0.983	0.981	0.984	0.990	0.996
	(0.008)	(0.004)	(0.000)	(0.001)	(0.027)
π_{ss}	1.021	1.021	1.034	1.018	1.024
	(0.012)	(0.004)	(0.002)	(0.003)	(0.007)
$\sigma_{\mu_z} \times 100$	0.330	0.378	0.403	0.297	0.609
	(0.013)	(0.072)	(0.039)	(0.003)	(0.342)
σ_d	0.127	0.122	0.152	0.033	0.053
	(0.058)	(0.008)	(0.006)	(0.010)	(0.114)
σ_n	0.044	0.064	0.087	0.035	0.108
	(0.017)	(0.010)	(0.007)	(0.002)	(0.111)
$\sigma_{\pi^*} \times 100$	0.043	0.060	0.247	0.083	0.086
	(0.036)	(0.016)	(0.042)	(0.001)	(0.075)
$\sigma_a \times 100$	0.236	0.218	0.677	0.395	0.148
	(0.129)	(0.043)	(0.039)	(0.021)	(0.509)
Additional Info					
Timing Premium	2.81%	2.77%	4.65%	7.33%	1.13%
IES	0.06	0.06	0.03	0.07	0.02
RRA	10	10	10	34.70	10
u_0	–459	–273	–5,945	0	–913,824

https://doi.org/10.1017/S0022109025000079 Published online by Cambridge University Press

FIGURE 1
Model Fit

Figure 1 shows the observables in the data along with the model-implied values at the state estimates from the CDKF for the baseline model $\mathcal{M}^{M,CS}$, estimated on quarterly data from 1961 to 2019. The value of τ denotes the correlation between the empirical series and the model-implied series.



compared to the standard specification with $u_0 = 0$. As argued by Andreasen and Jørgensen (2020), this helps to keep the household's risk aversion at a low and plausible level.

The forward-looking central bank assigns more weight to stabilizing future inflation than economic activity with $\widehat{\phi}_\pi = 3.96$ and $\widehat{\phi}_{\Delta c} = 1.10$, which is a common finding in the literature. For the structural shocks, we find that permanent productivity shocks display low persistence with $\widehat{\rho}_{\mu_z} = 0.49$, showing that the model does not rely on a strong long-run risk component. In contrast, the inflation target is highly persistent with $\widehat{\rho}_{\pi^*} = 0.995$ and it has low volatility with $\widehat{\sigma}_{\pi^*} = 0.00043$, implying that this shock captures long-run nominal risk. Finally, the preference shock, the labor supply shock, and the stationary productivity shock are also highly persistent with first-order autocorrelation functions of about 0.98.

Overall, the estimated structural parameters appear reasonable and consistent with micro evidence as well as previous findings for the New Keynesian model.

B. Model Fit

Figure 1 plots the data and the model-implied values (the thick line) for the 10 variables included in the estimation. The model captures the overall evolution in the labor supply $\widehat{l}_t$ and the real wage $\widehat{w}_t$ remarkably well despite our parsimonious

https://doi.org/10.1017/S0022109025000079 Published online by Cambridge University Press

specification of the labor market. This is also evident from the correlation between the data series and the model-implied series as denoted by τ in the figure, which is 0.87 for the labor supply and 0.85 for the real wage. The model provides an even closer fit to consumption growth Δc_t and inflation π_t with $\tau = 0.98$. For the short rate r_t, we see an outlier around 1980, which is expected due to our choice of downweighting the importance of the short rate in the estimation during the monetary policy experiment. We also find that the model fits the short rate closely at the 0 lower bound as desired and that all remaining bond yields are well matched by the model.

Accordingly, the proposed model with just five structural shocks provides a good in-sample fit to the 10 variables in $\mathbf{y}_t^{obs}$. To benchmark this result to the literature, recall that the New Keynesian model is typically estimated using as many shocks as observables. However, the dynamics of the yield curve is well captured by the first two principal components, implying that six structural shocks should be needed in our case. The fact that the proposed model matches the observed data using just five shocks is, therefore, very satisfying.

C. Unconditional Stylized Moments

Table 2 explores the ability of $\mathcal{M}^{M,CS}$ to match the unconditional means and standard deviations in $\mathbf{y}_t^{obs}$ as included when estimating $\mathcal{M}^{M,CS}$. The first column in Table 2 shows U.S. sample moments and their bootstrapped 95% confidence bands, while the second column shows the corresponding population moments in $\mathcal{M}^{M,CS}$. We first note that $\mathcal{M}^{M,CS}$ reproduces the mean of inflation and the mean of all bond yields. For instance, the level of the 3-month yield is 4.80% versus 4.58% in the data, and the level of the 10-year bond yield is 6.42% versus 6.13% in the data. This implies that the average yield spread is 162 basis points in $\mathcal{M}^{M,CS}$ compared to 155 basis points in U.S. data.

The model is also successful in matching the standard deviation of the labor supply (2.78% vs. 2.88% in the data), the real wage (1.99% vs. 2.20% in the data), consumption growth (1.60% vs. 1.74% in the data), and inflation (2.58% vs. 2.43% in the data). The standard deviations of all bond yields are also well matched.[14]

Accordingly, $\mathcal{M}^{M,CS}$ explains the overall level and variability of the data. This shows that the satisfying in-sample fit in Figure 1 does not come at the expense of distorted unconditional model dynamics. This indicates that the estimated state innovations $\widehat{\boldsymbol{\epsilon}}_{t+1}$ evolve according to the assumed laws of motion in equation (10) and hence do not show evidence of overfitting. We draw the same conclusion from an inspection of $\widehat{\boldsymbol{\epsilon}}_{t+1}$, which are basically uncorrelated as desired. For instance, the average of the absolute correlations between the five innovations is just 0.12, and the highest and lowest correlations are just 0.26 and −0.21, respectively.[15]

[14]Following the work of Piazzesi and Schneider (2007), the correlation between π_t and Δc_t has attracted some attention in the literature. We find $corr(\pi_t, \Delta c_t) = -0.16$ in $\mathcal{M}^{M,CS}$ and $corr(\pi_t, \Delta c_t) = -0.11$ in our quarterly sample from 1961 to 2019.

[15]The full correlation matrix for the structural innovations are reported in the Supplementary Material.

https://doi.org/10.1017/S0022109025000079 Published online by Cambridge University Press

TABLE 2

Unconditional First and Second Moments

The data moments shown in Table 2 are for the U.S. from 1961 to 2019 with 95% confidence bands stated below. These bands are computed using a block bootstrap with 10,000 bootstrap samples using blocks of 60 observations. The model-implied moments are computed in closed form using the procedure in Andreasen et al. (2018). The version of the model is denoted by the superscipts "M" for applying shrinkage to the unconditional moments and "CS" to the Campbell-Shiller moments. The subscript on the model object indicates that the standard specification of recursive preferences (EZ) is used in column 5 and that a third-order perturbation approximation (3th) to the model solution is used in column 6. All means and standard deviations are stated in annualized percentage, except for the standard deviation of $\widehat{l}_t$ and $\widehat{w}_t$ which are not annualized.

	Data	$\mathcal{M}^{M,CS}$	$\mathcal{M}^{M}$	$\mathcal{M}$	$\mathcal{M}^{M,CS}_{EZ}$	$\mathcal{M}^{M,CS}_{3th}$
	1	2	3	4	5	6
Means						
Δc_t	1.91 (1.39,2.44)	1.91	1.91	1.91	1.91	1.91
π_t	3.67 (1.93,5.41)	3.67	3.64	7.14	3.72	3.71
r_t	4.58 (2.21,6.96)	4.80	4.74	–1.92	4.78	4.54
$r_t^{(4)}$	5.04 (2.50,7.59)	4.93	4.97	–1.27	4.96	4.73
$r_t^{(12)}$	5.43 (2.91,7.95)	5.26	5.33	–0.26	5.44	5.25
$r_t^{(20)}$	5.70 (3.27,8.14)	5.58	5.61	0.26	5.79	5.64
$r_t^{(28)}$	5.91 (3.56,8.26)	5.91	5.88	0.66	6.04	5.97
$r_t^{(40)}$	6.13 (3.87,8.39)	6.42	6.29	1.24	6.29	6.38
Stds						
$\widehat{l}_t$	2.88 (2.42,3.34)	2.78	2.91	6.49	2.91	2.36
$\widehat{w}_t$	2.20 (1.65,2.75)	1.99	2.09	6.51	1.93	1.81
Δc_t	1.74 (1.49,1.98)	1.60	1.75	2.16	1.70	1.68
π_t	2.43 (1.18,3.67)	2.58	2.48	6.09	2.76	2.34
r_t	3.19 (2.07,4.32)	3.11	3.30	7.97	3.07	3.76
$r_t^{(4)}$	3.31 (2.16,4.46)	3.13	3.24	7.71	3.02	3.67
$r_t^{(12)}$	3.17 (2.02,4.32)	3.13	3.10	7.09	2.89	3.46
$r_t^{(20)}$	3.02 (1.89,4.15)	3.10	2.97	6.47	2.80	3.25
$r_t^{(28)}$	2.90 (1.78,4.01)	3.06	2.86	5.91	2.74	3.05
$r_t^{(40)}$	2.78 (1.68,3.88)	3.02	2.72	5.19	2.68	2.79

D. Ordinary Campbell-Shiller Loadings

Another important question is whether $\mathcal{M}^{M,CS}$ can match the empirical pattern in the ordinary Campbell-Shiller loadings β_k from equation (14), which we include in the estimation. Panel A in Table 3 reports these loadings in the sample along with their bootstrapped 95% confidence bands. A very encouraging finding is that $\mathcal{M}^{M,CS}$ generates ordinary Campbell-Shiller loadings that are *negative* and track

https://doi.org/10.1017/S0022109025000079 Published online by Cambridge University Press

TABLE 3

Ordinary and Risk-Adjusted Campbell-Shiller Loadings

Panel A in Table 3 shows the ordinary Campbell-Shiller regression loadings β_k for $m=4$. The empirical values are computed using quarterly U.S. data from 1961 to 2019, with the 95% confidence interval provided in parentheses, computed using a block bootstrap where the regressand and the regressor in equation (14) are sampled jointly in blocks of 10 observations in 10,000 bootstrap samples. The model-implied Campbell-Shiller loadings are computed in closed form. Panel B shows the risk-adjusted Campbell-Shiller regression loadings β_k^{Adj} for $m=4$ in quarterly U.S. data from 1961 to 2019 when using term premia from the particular version of the model with the 95% confidence interval provided in parentheses, computed using a block bootstrap where the regressand and the regressor in equation (15) are sampled jointly in blocks of 10 observations in 10,000 bootstrap samples.

	Data	$\mathcal{M}^{M,CS}$	$\mathcal{M}^{M}$	$\mathcal{M}$	$\mathcal{M}_{FZ}^{M,CS}$	$\mathcal{M}_{3th}^{M,CS}$
	1	2	3	4	5	6
Panel A. Ordinary CS Loadings						
β_{12}	–1.03 (–2.27,0.20)	–0.73	–0.28	0.49	–0.60	–0.72
β_{20}	–1.53 (–2.92,–0.14)	–0.74	–0.29	0.31	–0.36	–0.65
β_{28}	–1.93 (–3.43,–0.42)	–0.78	–0.30	0.20	–0.18	–0.64
β_{40}	–2.39 (–4.09,–0.70)	–0.82	–0.29	0.10	–0.01	–0.62
Panel B. Adjusted CS Loadings						
β_{12}^{Adj}	–	–0.50 (–1.57,0.99)	–0.33 (–1.41,1.21)	–0.57 (–1.78,1.35)	–0.90 (–1.93,0.57)	–0.04 (–1.73,1.65)
β_{20}^{Adj}	–	–0.49 (–1.74,1.23)	–0.34 (–1.58,1.36)	–0.59 (–1.72,1.11)	–1.42 (–2.60,0.20)	0.16 (–1.74,2.07)
β_{28}^{Adj}	–	–0.42 (–1.85,1.40)	–0.31 (–1.68,1.45)	–0.56 (–1.64,0.99)	–1.88 (–3.17,–0.15)	0.39 (–1.69,2.47)
β_{40}^{Adj}	–	–0.27 (–2.08,1.74)	–0.21 (–1.86,1.70)	–0.42 (–1.47,1.01)	–2.40 (–3.92,–0.52)	0.77 (–1.61,3.14)

the empirical loadings remarkably well inside their 95% confidence bands, although the loadings in the model do not fall as much with time to maturity as in the data. This shows that the model satisfies the first requirement for a correct specification of term premia.

E. Risk-Adjusted Campbell-Shiller Loadings

Next, we study moments that are not included in the estimation of $\mathcal{M}^{M,CS}$. A correct specification of term premia should imply that historical risk-adjusted bond yields satisfy the expectations hypothesis. Dai and Singleton (2002) show that this corresponds to testing whether the loading β_k^{Adj} is equal to 1 in the following version of the Campbell-Shiller regression

$$r_{t+m}^{(k-m)} - r_t^{(k)} - \left(TP_{t+m}^{(k-m)} - TP_t^{(k-m)}\right) + \frac{m}{k-m} TP_t^{fwd,(k-m)} = \alpha_k^{Adj} + \beta_k^{Adj} \frac{m}{k-m}\left(r_t^{(k)} - r_t^{(m)}\right) + u_{t+m,k}^{Adj}, \tag{15}$$

where term premia are subtracted from long-term yields. Here, the variable $TP_t^{fwd,(k)} = f_{t,k} - \mathbb{E}_t[r_{t+k}]$ is the term premium in the forward rate $f_{t,k} \equiv$

https://doi.org/10.1017/S0022109025000079 Published online by Cambridge University Press

$-\log\left(B_t^{(k+1)}/B_t^{(k)}\right)$ and $u_{t+m,k}^{Adj}$ is an error term. That is, we substract the estimated term premia by the New Keynesian model from U.S. bond yields $r_{t+m}^{(k-m)} - r_t^{(k)}$ and regress them on a constant and the yield spread in the U.S.

Panel B in Table 3 uses term premia from $\mathcal{M}^{M,CS}$ to compute risk-adjusted Campbell-Shiller loadings β_k^{Adj} and their 95% confidence bands on the historical sample from 1961 to 2019. We find that these risk-adjusted loadings β_k^{Adj} are notably larger than the corresponding unadjusted loadings β_k, and hence closer to the desired value of 1. For instance, at the 10-year maturity, the loading increases from $\beta_{40} = -2.39$ to $\beta_{40}^{Adj} = -0.27$. At the other maturities, we also find that the risk-adjusted Campbell-Shiller loadings are slightly below 0, but that the desired value of 1 generally is within the 95% confidence bands for β_k^{Adj}. The only exception is at the 1-year maturity, where the upper bound for the confidence interval is 0.99 and hence just below 1. Subject to this minor qualification, term premia from the model are not rejected by the data, implying that $\mathcal{M}^{M,CS}$ also passes the second requirement for a correct specification of term premia.

F. Inflation News in Bond Yields

Duffee (2018) shows that the quarterly news in bond yields $\tilde{r}_t^{(k)} = r_t^{(k)} - \mathbb{E}_{t-1}\left[r_t^{(k)}\right]$ is much more volatile than the quarterly news in expected inflation $\eta_{\pi,t}^{(k)} = \mathbb{E}_t\left[\frac{1}{k}\sum_{i=1}^{k}\pi_{t+i}\right] - \mathbb{E}_{t-1}\left[\frac{1}{k}\sum_{i=1}^{k}\pi_{t+i}\right]$. The inflation variance ratio $VR_\pi^{(k)} = \mathrm{V}\left[\eta_{\pi,t}^{(k)}\right]/\mathrm{V}\left[\tilde{r}_t^{(k)}\right]$ is therefore only around 0.15 in the U.S., whereas this ratio often exceeds 1 in various versions of the New Keynesian model (see Duffee (2018)). However, the time series for $\tilde{r}_t^{(k)}$ and $\eta_{\pi,t}^{(k)}$ in the U.S. display clear evidence of time-varying volatility, and Gomez-Cram and Yaron (2021) therefore refine the estimates in Duffee (2018) by correcting for heteroskedasticity. This increases $VR_\pi^{(k)}$ to 0.23, 0.22, and 0.19 at the 1-, 3-, and 5-year maturity, as shown in Table 4.[16]

The proposed model $\mathcal{M}^{M,CS}$ implies that the standard deviation in news to expected inflation is only 0.31 at the 1-year maturity, and falls steadily to 0.26 at the 5- and 10-year maturities. The standard deviation in news to bond yields is substantially higher at 0.49 at the 1-year maturity and 0.46 at the 3- and 5-year maturities, and hence within the reported 90% uncertainty bands for the corresponding data moments in Table 4. The model therefore implies fairly low inflation variance ratios of 0.41, 0.35, and 0.33 at the 1-, 3-, and 5-year maturities, respectively, which are just outside the reported 90% uncertainty bands. This shows that the proposed New Keynesian model goes a long way in addressing the critique of Duffee (2018). As with the risk-adjusted Campbell-Shiller loadings in Section IV.E, we emphasize that the model's ability to explain the inflation variance ratios is an out-of-sample test, in the sense that β_k^{Adj} and $VR_\pi^{(k)}$ are not included in the model estimation.

[16]We are grateful to Roberto Gomez-Cram for sharing these data moments.

https://doi.org/10.1017/S0022109025000079 Published online by Cambridge University Press

TABLE 4

News to Inflation and Bond Yields

Table 4 reports the annualized standard deviation of quarterly news in expected inflation $\eta_{\pi,t}^{(k)} = \mathbb{E}_t\left[\frac{1}{k}\sum_{i=1}^{k}\pi_{t+i}\right] - \mathbb{E}_{t-1}\left[\frac{1}{k}\sum_{i=1}^{k}\pi_{t+i}\right]$ in percentage, the annualized standard deviation of quarterly news in bond yields $\tilde{r}_t^{(k)} = r_t^{(k)} - \mathbb{E}_{t-1}\left[r_t^{(k)}\right]$ in percentage, and the inflation variance ratio $VR_{\pi}^{(k)} = \mathbb{V}\left[\eta_{\pi,t}^{(k)}\right]/\mathbb{V}\left[\tilde{r}_t^{(k)}\right]$. The data moments are from Gomez-Cram and Yaron (2021) (supported material provided by R. Gomez-Cram) with a correction for heteroskedasticity. These estimates are from 1962:Q1 to 2018:Q4, where the standard deviations in bond yields news use martingale forecasts, and the standard deviations in expected inflation news are obtained using the GDP deflator and surveys on current-quarter inflation. Figures in parentheses denote the 90% credibility interval. The corresponding model-implied moments are computed for the indicated versions of the New Keynesian model using a simulated sample of 100,000 observations to obtain the reported moments.

	Data	$\mathcal{M}^{M,CS}$	$\mathcal{M}^{M}$	$\mathcal{M}$	$\mathcal{M}_{EZ}^{M,CS}$	$\mathcal{M}_{3th}^{M,CS}$
	1	2	3	4	5	6
Std of Inflation News						
1-year	0.22 [0.19,0.25]	0.31	0.39	0.94	0.27	0.37
3-year	0.21 [0.18,0.24]	0.27	0.35	0.88	0.27	0.34
5-year	0.20 [0.18,0.23]	0.26	0.34	0.85	0.27	0.32
10-year	–	0.26	0.31	0.77	0.27	0.28
Std of Yield News						
1-year	0.46 [0.41,0.51]	0.49	0.62	1.86	0.48	0.45
3-year	0.44 [0.40,0.50]	0.46	0.56	1.39	0.43	0.44
5-year	0.46 [0.41,0.51]	0.46	0.53	1.24	0.39	0.43
10-year	–	0.45	0.48	1.01	0.33	0.41
Inflation Variance Ratio						
1-year	0.23 [0.16,0.32]	0.41	0.39	0.26	0.32	0.67
3-year	0.22 [0.16,0.32]	0.35	0.40	0.40	0.39	0.59
5-year	0.19 [0.14,0.27]	0.33	0.41	0.47	0.48	0.55
10-year	–	0.33	0.42	0.58	0.69	0.48

G. Term Premia

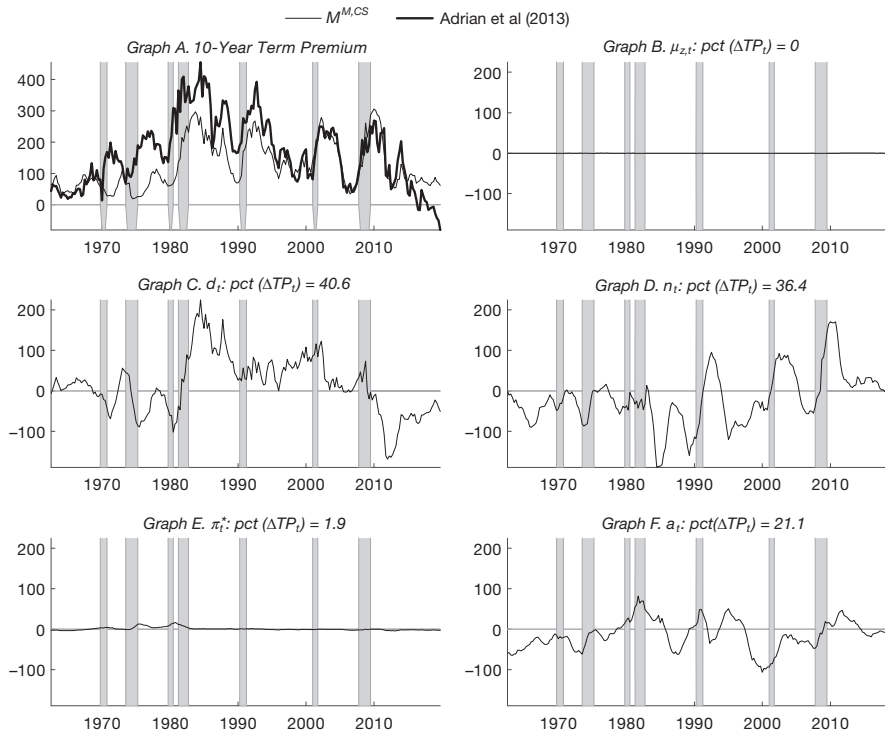
The 10-year term premium implied by $\mathcal{M}^{M,CS}$ is shown in Graph A of Figure 2, where the shaded bars denote NBER recessions. The graph reveals that the model generates the same overall pattern for the 10-year nominal term premium as found in the flexible 5-factor model of Adrian, Crump, and Moench (2013), which is a standard reduced-form Gaussian DTSM without any economic structure. The correlation between the two measures of term premium is 0.73, with the similarities being particularly strong since the early 1980s. Note also that both measures generally increase during NBER recessions and hence capture the counter-cyclical nature of term premia, with the two recessions during the 1970s as the main exceptions for $\mathcal{M}^{M,CS}$. The summary statistics for term premia are also very similar across the two models, as the 10-year nominal term premium

https://doi.org/10.1017/S0022109025000079 Published online by Cambridge University Press

FIGURE 2

The 10-year Term Premium

Graph A in Figure 2 shows the 10-year term premium in $\mathcal{M}^{M,CS}$ and in the model by Adrian et al. (2013). Graphs B F show how each of the structural shocks in $\mathcal{M}^{M,CS}$ contribute to the variation in the 10-year term premium. The percentage of the total variation in the term premium explained by each shock, denoted pct(ΔTP_t), is computed using equation (16) based on the absolute variation in the series. The gray shaded bars denote NBER recessions, and term premium is expressed in annualized basis points.



in the model of Adrian et al. (2013) has a mean of 163 basis points and a standard deviation of 110 basis points, while the corresponding moments in $\mathcal{M}^{M,CS}$ are 151 and 100 basis points, respectively, in a simulated sample of 100,000 observations.

To conduct a shock decomposition of the 10-year term premium, we condition on the nonlinear solution in equation (12) obtained using all five shocks and adopt the following procedure. First, let $TP_t^{(k),all}$ denote the term premium computed using the nonlinear solution and the estimated states $\widehat{\mathbf{x}}_t$ from the CDKF using all shocks. Second, let $TP_t^{(k),-i}$ denote the term premium when omitting variation in $\widehat{\mathbf{x}}_t$ due to the ith shock. The contribution to term premium by the ith shock is then $\Delta TP_t^{(k),i} \equiv TP_t^{(k),all} - TP_t^{(k),-i}$, which we plot in Figure 2 for each of the five shocks. To quantify the variation explained by a given shock, we compute the percentage of the total variation in the term premium explained by each shock as

https://doi.org/10.1017/S0022109025000079 Published online by Cambridge University Press

$$\text{pct}(TP_t^{(k),i}) = \frac{\sum_{t=1}^{T} |\Delta TP_t^{(k),i} - \overline{\Delta TP}^{(k),i}|}{\sum_{i=1}^{n_\varepsilon} \sum_{t=1}^{T} |\Delta TP_t^{(k),i} - \overline{\Delta TP}^{(k),i}|} \quad \text{for } i = \{1, 2, \ldots, n_\varepsilon\}, \tag{16}$$

where $\overline{\Delta TP}^{(k),i}$ denotes the sample average of $\Delta TP_t^{(k),i}$. We find that demand and labor supply shocks are the two dominating forces, explaining 41% and 36%, respectively, of the variation in the 10-year term premium. Stationary productivity shocks account for 21%, whereas shocks to the inflation target π_t^* and the growth rate $\mu_{z,t}$ have hardly any effect on the 10-year term premium. The decomposition also shows that the elevated level of the term premium during the two recessions in the early 1980s are due to demand and stationary productivity shocks. For the 1991 and the 2001 recessions, labor supply shocks and stationary productivity shocks are the main drivers behind the term premium. More recently, we see that demand, labor supply, and stationary productivity shocks all contribute to generate a high term premium during the 2007–2009 Great Recession.

H. Understanding the Key Mechanisms in the Model

At this point, we have shown that the proposed model i) explains historical bond yields, ii) matches unconditional properties of the data, iii) passes the two requirements for a correct specification of term premia, and iv) goes a long way in matching the level of news in expected inflation. Most of these features are also matched by reduced-form DTSMs, but these models offer little insights into the economic mechanisms that determine bond yields and especially term premia. The model we propose provides such a structural explanation, and this section analyzes the key mechanisms in $\mathcal{M}^{M,CS}$ that drive term premia. Our discussion is structured around Table 5, which shows how unconditional moments and Campbell-Shiller loadings (both ordinary and risk-adjusted) are affected when omitting one of the five shocks in the model.

We first note that permanent productivity shocks have a large impact on the level of bond yields, as omitting variation in $\mu_{z,t}$ (i.e., $\sigma_{\mu_z} = 0$) increases the average level of the yield curve by about five percentage points. For instance, the mean of the 10-year yield increases from 6.42% with all five shocks to 11.60% when omitting permanent productivity shocks. This effect arises from a precautionary saving motive, as omitting permanent productivity shocks make the economy less risky and this reduces the negative precautionary saving correction in bond yields. We also note that omitting permanent productivity shocks reduce the standard deviations in the three macro variables $\widehat{l}_t$, $\widehat{w}_t$, and Δc_t, whereas the variability in π_t is almost unaffected. On the other hand, the standard deviation in bond yields actually increase when imposing that $\sigma_{\mu_z} = 0$. This may at first seem counter-intuitive, but this effect arises because the nonlinear policy function for bond yields changes with $\sigma_{\mu_z} = 0$ such that they depend more strongly on the other structural shocks due to a sizable risk-adjustment in the model solution. The ordinary and risk-adjusted Campbell-Shiller loadings are not materially affected by letting $\sigma_{\mu_z} = 0$. This suggests that permanent productivity shocks are not the key source for

https://doi.org/10.1017/S0022109025000079 Published online by Cambridge University Press

TABLE 5

Decomposing the Effects of the Structural Shocks

Table 5 reports unconditional moments for $\mathcal{M}^{M,CS}$ when all structural shocks are present in column 1, and when each of the structural shocks are omitted in columns 2 to 6. The model-implied moments are computed in closed form using the procedure in Andreasen et al. (2018). All means and standard deviations are stated in annualized percentage, except for the standard deviation of $\widehat{l}_t$ and $\widehat{w}_t$, which are not annualized.

	$\mathcal{M}^{M,CS}$	$\sigma_{\mu_z}=0$	$\sigma_{cl}=0$	$\sigma_{\eta}=0$	$\sigma_{\pi^*}=0$	$\sigma_{a}=0$
	1	2	3	4	5	6
Means						
Δc_t	1.91	1.91	1.91	1.91	1.91	1.91
π_t	3.67	4.70	7.00	3.76	3.67	3.66
r_t	4.80	9.27	18.43	5.34	4.76	3.56
$r_t^{(4)}$	4.93	9.45	18.43	5.51	4.88	3.51
$r_t^{(12)}$	5.26	9.92	18.51	5.96	5.20	3.58
$r_t^{(20)}$	5.58	10.40	18.54	6.37	5.51	3.85
$r_t^{(28)}$	5.91	10.88	18.56	6.77	5.83	4.22
$r_t^{(40)}$	6.42	11.60	18.57	7.37	6.34	4.91
Stds						
$\widehat{l}_t$	2.78	1.82	1.81	1.51	2.78	4.47
$\widehat{w}_t$	1.99	1.30	1.32	1.52	1.98	2.90
Δc_t	1.60	0.80	1.42	1.44	1.60	1.88
π_t	2.58	2.50	2.44	2.45	0.82	3.61
r_t	3.11	3.49	2.66	2.84	1.77	5.16
$r_t^{(4)}$	3.13	3.45	2.60	2.97	1.85	3.97
$r_t^{(12)}$	3.13	3.41	2.51	3.07	1.93	3.33
$r_t^{(20)}$	3.10	3.39	2.45	3.08	1.93	3.24
$r_t^{(28)}$	3.06	3.37	2.39	3.07	1.94	3.25
$r_t^{(40)}$	3.02	3.36	2.30	3.05	1.96	3.34
Ordinary CS Loadings						
β_{12}	–0.73	–0.51	1.02	–0.87	–0.74	–0.62
β_{20}	–0.74	–0.70	1.03	–1.07	–0.76	–0.55
β_{28}	–0.78	–0.78	1.03	–1.24	–0.81	–0.57
β_{40}	–0.82	–0.83	1.04	–1.40	–0.87	–0.62
Adjusted CS Loadings						
β_{12}^{Adj}	–0.50	–0.63	–0.99	–0.93	–0.61	–0.29
β_{20}^{Adj}	–0.49	–0.76	–1.49	–1.59	–0.79	–0.13
β_{28}^{Adj}	–0.42	–0.76	–1.89	–2.15	–0.93	0.03
β_{40}^{Adj}	–0.27	–0.58	–2.35	–2.85	–1.07	0.26

generating bond return predictability and hence variability in term premia, consistent with the results in Figure 2.

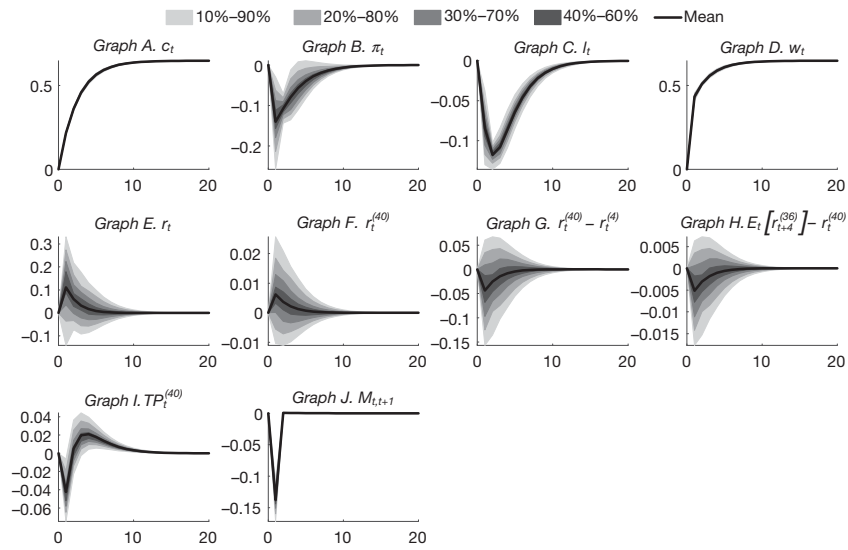
To further analyze the effects a change in productivity, Figure 3 shows the generalized IRFs following a positive 1-standard-deviation permanent productivity shock. These IRFs depend on the initial state $\mathbf{x}_t$ when the shock hits in period $t+1$, and we therefore show fan charts for the distribution of these responses across 1,000 randomly generated initial states from a simulated sample of the model. Consistent with the results in Table 5, the 10-year term premium is basically unaffected by this shock. On the other hand, consumption and the wage level increase strongly, whereas inflation shows a small reduction. These findings are consistent with the empirical evidence provided in Altig, Christiano, Eichenbaum, and Linde (2011) using quarterly U.S. data from 1982 to 2008. However, the drop in the labor supply in Figure 3 is contrary to the finding in Altig et al. (2011), but Fisher (2006) shows that the reponse in the labor supply is sensitive to the considered sample, as it is negative when using data before 1982 but positive when using data after 1982.

https://doi.org/10.1017/S0022109025000079 Published online by Cambridge University Press

FIGURE 3

Impulse Response Functions: A Permanent Productivity Shock

Figure 3 shows the generalized impulse response functions (IRFs) for a positive 1-standard-deviation shock to $\mu_{z,t}$, where the various shadings cover the indicated fraction of the distribution for these IRFs obtained using 1,000 randomly generated initial states. The IRFs are computed in closed form for the second order projection solution using the approach in Andreasen et al. (2018), except for $M_{t,t+1}$, which is computed using Monte Carlo integration with 1,000 draws. Except for the term premium $TP_t^{(40)}$ and the nominal stochastic discount factor $M_{t,t+1}$, all impulse response functions are expressed in percentage deviations (i.e., scaled by 100) from the steady state or from the deterministic growth path (in the case of consumption and the wage level). All bond yields and inflation are measured in annualized terms and the term premium $TP_t^{(40)}$ is expressed in annualized basis points.



Accordingly, the IRFs to a permanent productivity shock appear consistent with existing empirical evidence. This suggests that the shock is well specified in the model, and that its responses do not appear to be distorted by letting z_t enter in the utility function in equation (2).

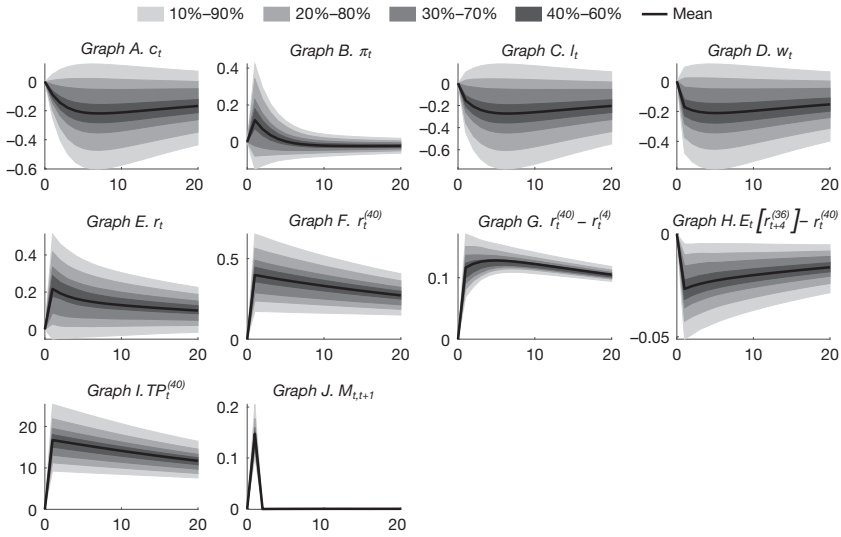
Our second observation is that demand shocks generate an upward sloping yield curve. This is seen from the third column in Table 5, which shows an almost flat yield curve close to the steady state of 18.50% when omitting demand shocks (i.e., $\sigma_d = 0$). In contrast, demand shocks often generate a downward sloping yield curve in other versions of the New Keynesian model (see, for instance, Nakata and Tanaka (2016)). To understand this implication of $\mathcal{M}^{M,CS}$, consider the IRFs in Figure 4 for a positive demand shock. We generally find that inflation π_t and the long-term bond yield $r_t^{(40)}$ increase, and hence that $B_t^{(40)}$ falls following a demand shock. On the other hand, the responses of consumption, labor supply, and the real wage may be either positive or negative. In contrast, when solving the model without accounting for risk (as typically done in the macro literature), we find almost exclusively positive responses in consumption, the labor supply, and the real wage to a demand shock, as shown in the Supplementary Material. This means that the sizable risk-adjusted required in the model to match bond yields has notable macroeconomic effects. Despite these state-dependent responses, we see a large

https://doi.org/10.1017/S0022109025000079 Published online by Cambridge University Press

FIGURE 4

Impulse Response Functions: A Demand Shock

Figure 4 shows the generalized IRFs for a positive 1-standard-deviation shock to d_t, where the various shadings cover the indicated fraction of the distribution for these IRFs obtained using 1,000 randomly generated initial states. The IRFs are computed in closed form for the second order projection solution using the approach in Andreasen et al. (2018), except for $M_{t,t+1}$, which is computed using Monte Carlo integration with 1,000 draws. Except for the term premium $TP_t^{(40)}$ and the nominal stochastic discount factor $M_{t,t+1}$, all impulse response functions are expressed in percentage deviations (i.e., scaled by 100) from the steady state or from the deterministic growth path (in the case of consumption and the wage level). All bond yields and inflation are measured in annualized terms and the term premium $TP_t^{(40)}$ is expressed in annualized basis points.



increase in the nominal stochastic discount factor $M_{t.t+1}$ due to $d_{t+1}/d_t > 1$ and an increase in $\left(\mathbb{E}_t\left[V_{t+1}^{1-\alpha}\right]\right)^{\frac{\alpha}{1-\alpha}}/V_{t+1}^{\alpha}$. As shown in Rudebusch and Swanson (2012), such a negative comovement between $M_{t,t+1}$ and the bond price $B_t^{(40)}$ over the lifetime of the bond generates a positive term premium. Thus, demand shocks make long-term bonds a risky investment for the household, and this explains why they generate a strong increase in the 10-year term premium $TP_t^{(40)}$ of about 15 basis points and an upward sloping yield curve.

Another important observation from Figure 4 is that demand shocks increase the yield spread $r_t^{(40)} - r_t^{(4)}$ and reduce the expected change in the long yield $\mathbb{E}_t\left[r_{t+4}^{(36)}\right] - r_t^{(40)}$. Demand shocks, therefore, also help to generate the desired negative estimates of $\beta^{(k)}$ in the ordinary Campbell-Shiller regressions. Indeed, the ordinary Campbell-Shiller loadings are basically 1 without demand shocks, and the model-implied risk adjustment in U.S. bond yields is negligible with risk-adjusted Campbell-Shiller loadings that almost coincide with the unadjusted slope coefficients in the first column in Table 3. This shows that demand shocks are a key driver for generating return predictability and variation in term premia in the model. Hence, when omitting these shocks, we greatly reduce the variation in term premia and therefore also the standard deviation in bond yields, as shown in the third column in Table 5. In contrast, the standard deviation of inflation only drops slightly from 2.58% to 2.44% without demand shocks. These shocks, therefore, help to explain the

https://doi.org/10.1017/S0022109025000079 Published online by Cambridge University Press

https://doi.org/10.1017/S0022109025000079 Published online by Cambridge University Press

variation in bond yields without materially affecting inflation, which is precisely what is required to match the low inflation variance ratios discussed in Section IV.F. Indeed, the inflation variance ratio for the 10-year bond yield increases from 0.33 to 0.65 without demand shocks in the model.

Given the importance of the demand shock for the New Keynesian model to match bond yields, we briefly explore how well this shock relates to the widely used consumer sentiment index from the University of Michigan. This index is obtained by surveying a cross-section of the population in the U.S. to capture their views about the current state of their own finances and the U.S. economy in general. The index, therefore, responds to aggregate shocks hitting the U.S. economy such as changes in productivity and government spendings but also to variation within the household that are unrelated to such external shocks, as discussed in Lagerborg, Pappa, and Ravn (2023). This means that we should not expect a perfect correlation between this sentiment index and our measure of the demand shock. A regression of the consumer sentiment index on a constant and the estimated demand shock $\widehat{d}_t$ from $\mathcal{M}^{M,CS}$ shows a positive correlation of 0.42, with a 95% confidence interval of $(0.24,0.59)$ obtained using Newey-West standard errors with 4 lags. This shows that the demand shock is not simply some unobserved statistical factor extracted to fit bond yields, but instead is well connected to the level of consumer sentiment in the U.S. and hence has a clear economic interpretation.

The last columns in Table 5 show that i) labor supply shocks n_t unsurprisingly explain much of the variation in the labor supply, ii) shocks to π_t^* control much of the variation in inflation and bond yields, and that iii) stationary productivity shocks a_t mainly affect the level of bond yields and the variation in the labor supply, the real wage, inflation, and short-term bond yields.

V. Sensitivity Analysis

This section explores various aspects of the baseline model $\mathcal{M}^{M,CS}$ that are new to the literature. We first examine the effects of the estimator with shrinkage in Section V.A, while Section V.B applies the standard formulation of recursive preferences. Finally, we discuss the accuracy of the projection solution in Section V.C and relate it to the standard perturbation approximation.

A. The Effects of Shrinkage

The results presented so far are obtained when shrinking the traditional QML estimates of the structural parameters toward some stylized empirical moments for $\mathbf{y}_t^{obs}$. Given that this estimator is new to the literature on the New Keynesian model, we next explore the effects of gradually removing this form of shrinkage. We first re-estimate the model when only shrinking the QML estimates to the first and second unconditional moments of $\mathbf{y}_t^{obs}$ and not to the ordinary Campbell-Shiller loadings. This version of the model is denoted $\mathcal{M}^{M}$. Table 1 shows that this modification implies slightly higher curvature in the utility function ($\chi = 7.1$ vs. $\chi = 5.8$), lower price stickiness ($\xi_{Calvo} = 0.31$ vs. $\xi_{Calvo} = 0.44$), and a lower weight on consumption growth in the Taylor-rule ($\phi_{\Delta c} = 0.66$ vs. $\phi_{\Delta c} = 1.10$) when compared to $\mathcal{M}^{M,CS}$. The unconditional means and standard deviations in Table 2

https://doi.org/10.1017/S0022109025000079 Published online by Cambridge University Press

are basically unchanged, whereas the standard deviations of news to inflation and bond yields in Table 4 increase and imply larger inflation variance ratios in $\mathcal{M}^{M}$ than in $\mathcal{M}^{M,CS}$. We further find that $\mathcal{M}^{M}$ generates bond return predictability with ordinary Campbell-Shiller loadings around -0.3, which are somewhat lower (in absolute terms) than in $\mathcal{M}^{M,CS}$ and the data. The risk-adjusted Campbell-Shiller loadings for $\mathcal{M}^{M}$ increase slightly compared to $\mathcal{M}^{M,CS}$, with their 95% confidence bands including the desired value of 1, as seen from Table 3.

Another possibility is to abstract from any shrinkage and simply use QML for the estimation. We refer to this version of the model as $\mathcal{M}$. This modification gives somewhat larger changes in the estimated structural parameters in Table 1, with stronger habit formation ($b = 0.84$ vs. $b = 0.65$), less wage stickiness ($\kappa_w = 0.83$ vs. $\kappa_w = 0.92$), and a much larger weight on consumption growth in the Taylor-rule ($\phi_{\Delta c} = 4.57$ vs. $\phi_{\Delta c} = 1.10$) when compared with $\mathcal{M}^{M,CS}$. In addition, the standard deviations for all five structural shocks increase in $\mathcal{M}$ compared to $\mathcal{M}^{M,CS}$, which illustrates the tendency of QML to select large structural shocks in the New Keynesian model, as discussed in Section III.C. By construction, these estimates for $\mathcal{M}$ give a higher value of the log-likelihood function and therefore a closer in-sample fit than in both $\mathcal{M}^{M}$ and $\mathcal{M}^{M,CS}$ that apply shrinkage. However, Table 2 shows that $\mathcal{M}$ completely misses the i) mean of inflation, ii) the mean of bond yields, and iii) generates too much volatility in the observables $\mathbf{y}_t^{obs}$, with all standard deviations exceeding their 95% confidence bands. This imply that the standard deviations of news in expected inflation and bond yields are much larger than in the data according to Table 4. Thus, the standard QML estimates display clear signs of overfitting, as the improved value of the quasi log-likelihood function compared to $\mathcal{M}^{M,CS}$ and $\mathcal{M}^{M}$ comes at the cost of distorting the fit to several unconditional properties of the model. This also distorts estimates of term premia in $\mathcal{M}$, as its ordinary Campbell-Shiller loadings are all positive and outside of the 95% confidence bands for the corresponding sample moments according to Table 3.

We, therefore, conclude that shrinking in the estimation of the structural parameters is essential for the New Keynesian model to provide a satisfying in-sample fit and match several unconditional aspects of bond yields and macroeconomic variables.

B. Standard Formulation of Recursive Preferences

Our baseline model $\mathcal{M}^{M,CS}$ uses the flexible formulation of recursive preferences in Andreasen and Jørgensen (2020) with the utility constant u_0 to separate the IES, RRA, and the timing attitude. We next re-estimate the model with $u_0 = 0$ to recover the standard specification of recursive preferences applied in Rudebusch and Swanson (2012) and Binsbergen, Fernandez-Villaverde, Koijen, and Rubio-Ramirez (2012), among many others. We refer to this version of the model as $\mathcal{M}_{\text{EZ}}^{M,CS}$, which we estimate using the same shrinkage specification as in our baseline model. Table 1 shows that this seemingly minor modification implies substantial changes in the estimated structural parameters. In particular, we find stronger habit formation ($b = 0.87$ vs. $b = 0.65$), less curvature in the utility function ($\chi = 1.95$ vs. $\chi = 5.83$), much more price stickiness ($\xi_{Calvo} = 0.77$ vs. $\xi_{Calvo} = 0.44$), a larger weight on consumption growth in the Taylor-rule

($\phi_{\Delta c} = 2.98$ vs. $\phi_{\Delta c} = 1.10$), much smaller demand shocks ($\sigma_d = 0.033$ vs. $\sigma_d = 0.127$), and larger stationary productivity shocks ($\sigma_a = 0.0040$ vs. $\sigma_a = 0.0024$) when compared to $\mathcal{M}^{M,CS}$. As a result, we obtain a high RRA of 35 in $\mathcal{M}^{M,CS}_{\text{EZ}}$ with $\alpha = -16.49$, as typically found when estimating the New Keynesian model with recursive preferences.

The unconditional means and standard deviations in Table 2 are almost perfectly matched by $\mathcal{M}^{M,CS}_{\text{EZ}}$. However, Table 3 shows that the model is unable to reproduce the ordinary Campbell-Shiller loadings at the 7- and 10-year maturities, and it misses completely the risk-adjusted Campbell-Shiller loadings, which are far from the desired value of 1. These findings suggest that term premia are not appropriately specified in this version of the New Keynesian model. Finally, Table 4 shows that the inflation variance ratios increase monotonically with the time to maturity and clearly become too large. For instance, the inflation variance ratio is 0.48 and 0.69 at the 5- and 10-year maturity in $\mathcal{M}^{M,CS}_{\text{EZ}}$ but only 0.19 in U.S. data at the 5-year maturity.

To conclude, the flexible formulation of recursive preferences in Andreasen and Jørgensen (2020) is required to enable the New Keynesian model to appropriately capture the dynamics of bond yields and their embedded term premia.

C. Accuracy of the Model Solution

All versions of the New Keynesian model have, so far, been estimated using the second-order projection solution outlined in Section III.B. Table 6 studies the accuracy of this approximation on a grid of $S = 10{,}000$ simulated states and compare its performance to the standard perturbation approximation up to fifth order as made available by Levintal (2017). We report accuracy separately for the $n_m = 9$ equations defining the macro block of the model and the $n_b = 40$ equations defining bond prices. This is done using the standard summary statistics

$$\text{MAE} = \log 10\left(\frac{1}{nS}\sum_{s=1}^{S}\sum_{i=1}^{n}|EE_{i,s}|\right) \tag{17}$$

$$\text{RMSE} = \log 10\left(\frac{1}{n}\sum_{i=1}^{n}\sqrt{\frac{1}{S}\sum_{s=1}^{S}EE_{i,s}^2}\right)$$

$$\text{Max AE} = \log 10\left(\frac{1}{n}\sum_{i=1}^{n}\max\left(\{|EE_{i,s}|\}_{s=1}^{S}\right)\right)$$

for $n = n_m$ and $n = n_b$. Here, $EE_{i,s}$ is the ith unit-free Euler-equation error at state value $\boldsymbol{x}_s$, with $\log 10$ denoting the base 10 logarithm (e.g., $\log 10(0.01) = -2$).

Panel A in Table 6 considers the macro block of the baseline model $\mathcal{M}^{M,CS}$, where the second-order perturbation approximation clearly does better than the certainty equivalent first-order solution. However, accuracy does surprisingly not improve monotonically when increasing the approximaiton order for standard perturbation. Our second-order projection solution gives marginally higher accuracy than even a fifth order perturbation solution for the MAE and the RMSE (as indicated by the bold figures), whereas the second-order perturbation solution gives the lowest maximum absolute error. For the bond equations, we see larger differences between the two solution methods, where the second-order projection

https://doi.org/10.1017/S0022109025000079 Published online by Cambridge University Press

TABLE 6

Accuracy of Model Solutions

Table 6 shows the mean absolute errors (MAE), the root mean squared errors (RMSE), and the maximum absolute errors (Max AE) as defined in equation (17) for the nine equations defining the macro block of the New Keynesian model and for the 40 equations defining log-transformed bond prices for the 10-year yield curve. These accuracy measures are computed on a simulated grid of 10,000 observations obtained from the considered version of the model using a second-order perturbation approximation. Conditional expectations in Euler-equations are evaluated using Gauss-Hermite quadrature with five points for each of the five structural shocks, giving a total of 5^5 integration points for a given state value. A bold figure indicates the best performing model along a given accuracy measure for a given model.

		Perturbation					Projection
		1st	2nd	3rd	4th	5th	2nd
		1	2	3	4	5	6
Panel A. $\mathcal{M}^{M,CS}$							
Macro Eqs	MAE	−1.66	−2.59	−2.54	−2.78	−2.73	**−2.76**
	RMSE	−1.65	−2.48	−2.41	−2.46	−2.46	**−2.51**
	Max AE	−1.49	**−1.75**	−1.44	−1.26	−1.21	−1.47
Bond Eqs	MAE	−1.04	−2.12	−1.87	−2.09	−1.97	**−2.74**
	RMSE	−1.04	−2.00	−1.77	−1.79	−1.75	**−2.34**
	Max AE	−1.03	**−1.27**	−0.83	−0.61	−0.55	−1.21
Panel B. $\mathcal{M}^{M,CS}_{EZ}$							
Macro Eqs	MAE	−1.42	11.56	6.43	±∞	±∞	**−2.40**
	RMSE	−1.20	13.46	8.02	±∞	±∞	**−1.89**
	Max AE	−0.46	15.45	9.84	±∞	±∞	**−0.79**
Bond Eqs	MAE	−1.29	−1.07	−1.06	217.18	204.95	**−2.63**
	RMSE	−1.29	−0.46	−0.09	±∞	±∞	**−2.00**
	Max AE	−1.28	0.78	1.50	221.17	208.94	**−0.89**
Panel C. $\mathcal{M}^{M,CS}_{\sigma_d=0}$							
Macro Eqs	MAE	−1.75	−3.64	−3.60	−4.80	**−4.94**	−4.02
	RMSE	−1.75	−3.56	−3.57	−4.47	**−4.53**	−3.82
	Max AE	−1.63	−2.50	−2.58	−2.69	**−2.72**	−2.52
Bond Eqs	MAE	−1.12	−4.10	−3.17	−5.00	**−5.08**	−4.30
	RMSE	−1.12	−3.99	−3.17	−4.93	**−5.02**	−4.17
	Max AE	−1.12	−3.05	−3.10	−3.95	**−4.44**	−3.36

solution gives MAE= −2.74 and RMSE= −2.34, whereas we find −1.97 and −1.75, respectively, for a fifth order perturbation solution. Analogue to the macro block, we also note that the performance of standard perturbation for bond prices does not improve monotonically when increasing the approximation order.

Panel B considers $\mathcal{M}^{M,CS}_{EZ}$ with the standard specification of recursive preferences. The results show that the perturbation solution breaks down in this case, as the Euler-errors are very large and increase with the approximation order. In contrast, our second-order projection solution performs well also in this case.

To illustrate what drives this disappointing performance of the perturbation approximation, consider a restricted version of the baseline model without demand shocks by letting $\sigma_d = 0$. This parametrization is informative because it implies that the deterministic steady state is close to the unconditional mean (as shown for bond yields in Section IV.H), and the perturbation approximation should therefore perform well in this case. This is confirmed in Panel C of Table 6, as the fifth-order perturbation solution delivers a very high degree of accuracy in this case and clearly outperforms our second-order projection solution.

To show that the accuracy of the model solution has important consequences for the New Keynesian model, we finally re-estimate the model using a third-order perturbation solution, as widely applied in the literature (see Andreasen (2012) and

https://doi.org/10.1017/S0022109025000079 Published online by Cambridge University Press

https://doi.org/10.1017/S0022109025000079 Published online by Cambridge University Press

Rudebusch and Swanson (2012), among many others). This version of the model is denoted $\mathcal{M}_{3\text{rd}}^{M,CS}$. We find that this model performs well in matching the unconditional means and standard deviations in Table 2 and the Campbell-Shiller loadings in Table 3, but that the variance ratios in Table 4 are somewhat higher than with the projection solution. However, the structural parameters in Table 1 differ substantially from those obtained using the projection solution. For instance, with the third-order perturbation approximation, the subjective discount factor becomes very low ($\beta = 0.948$ vs. $\beta = 0.991$) and the curvature in the utility function becomes very high ($\chi = 15.63$ vs. $\chi = 5.83$) when compared to $\mathcal{M}^{M,CS}$. Also, the weight on inflation in the Taylor-rule ϕ_π becomes implausible large and hits the imposed upper bound of 10.

Accordingly, the proposed second-order projection solution delivers high accuracy and ensures sensible structural estimates, whereas the performance of standard perturbation deteriorates when the deterministic steady state is too far from the unconditional mean.

VI. Additional Model Implications

This section considers the baseline model $\mathcal{M}^{M,CS}$ and studies three additional aspects of the model that are not included in the estimation, and hence can be considered as representing over-identified restrictions. Joslin et al. (2014) criticize a wide class of macro-finance term structure models because they are unable to address the so-called "spanning puzzle." We summarize the arguments of Joslin et al. (2014) in Section VI.A and show that $\mathcal{M}^{M,CS}$ goes a long way in addressing this puzzle. The model's ability to capture the dynamics of real bond yields are examined in Section VI.B, while Section VI.C studies its implications for the price-dividend ratio and equity returns.

A. The Yield Curve and Spanned Macro Variation

Many DTSMs with macro variables imply that bond yields are a linear combination of latent factors and observed macro variables. This linear mapping can (up to knife-edge restrictions) be inverted to express macro variables as a function of bond yields. All variation in macro variables is therefore spanned (i.e., explained) by bond yields. However, this implication is heavily criticized by Joslin et al. (2014) because regressions of macro variables on linear combination of bond yields such as the principal components typically generate R^2 values substantially below 1. This constitutes the "spanning puzzle," which leads Joslin et al. (2014) to challenge the usefulness of most equilibrium models—including the standard New Keynesian model. The model we propose also implies that bond yields depend on macro variables, but this relation is not linear. Thus, the nonlinear structure of our model may generate what may appear to be unspanned variation in macro variables and hence resolve the spanning puzzle.

We explore this possibility in Table 7 by regressing each of the four macro variables included in the model estimation on the first K principal components of bond yields. The model $\mathcal{M}^{M,CS}$ has five structural shocks, suggesting that at least five principal components are required to span variation in the macro variables. The

TABLE 7

Regression Evidence on the Spanning Hypothesis

Table 7 shows the R^2 in percentage from the regression $m_t = \alpha + \beta' \mathbf{pca}_t^{(K)} + u_t$, where m_t refers to a macro variable and $\mathbf{pca}_t^{(K)}$ of dimension $K \times 1$ contains the first K principal components of bond yields. The R^2s in the data are provided in column 1 and computed on quarterly U.S. data from 1961 to 2019, with the 95% confidence interval (shown below the estimate) computed using a block bootstrap, where the regressand and the regressors are sampled jointly in blocks of 50 observations in 10,000 bootstrap samples. The corresponding R^2s implied by the New Keynesian model $\mathcal{M}^{M,CS}$ are computed using a simulated sample of 100,000 observations. The simulated sample in column 2 is obtained using the nonlinear model solution (i.e., second-order projection) and with measurement errors for macro variables and bond yields of the same size as considered in the estimation. The same nonlinear model solution is used in column 3, but no measurement errors are added to the macro variables and bond yields. The simulated sample in column 4 uses a simplified second-order projection solution, where all terms that are quadratic in the states are omitted.

	Data	Nonlinear Model & Measurement Errors	Nonlinear Model	Linear Model
	1	2	3	4
$K=5$				
$\widehat{l}_t$	26.23 (10.62,60.97)	32.39	51.58	88.92
$\widehat{w}_t$	16.53 (4.32,41.36)	34.18	73.74	94.61
Δc_t	30.40 (15.63,46.84)	3.44	18.76	74.06
π_t	64.08 (40.48,80.05)	84.57	86.36	98.95
$K=6$				
$\widehat{l}_t$	28.11 (11.42,63.42)	32.41	52.05	100.00
$\widehat{w}_t$	17.31 (5.44,42.89)	34.21	79.64	100.00
Δc_t	30.40 (16.53,47.02)	3.46	68.56	100.00
π_t	64.34 (40.82,80.50)	84.57	90.85	100.00

first column in Table 7 shows that U.S. bond yields only explain a fairly small proportion of the variation in the labor supply $\widehat{l}_t$ (26.2%), the real wage $\widehat{w}_t$ (16.5%), and consumption growth Δc_t (30.4%), whereas inflation π_t displays some evidence of spanning with an R^2 of 64.1%. The results for the New Keynesian model are very similar to these regressions according to the second column in Table 7, where the corresponding values of the R^2 are 32.4% for $\widehat{l}_t$, 34.2% for $\widehat{w}_t$, 3.4% for Δc_t, and 84.6% for π_t. These figures are computed using a simulated sample of 100,000 observations that include the same measurement errors $\mathbf{v}_t$ as applied when estimating $\mathcal{M}^{M,CS}$. Measurement errors help to generate unspanned variation, as emphasized in Bauer and Rudebusch (2017), and we, therefore, omit these errors in the third column in Table 7. The R^2 values then increase to 51.6% for $\widehat{l}_t$, 73.7% for $\widehat{w}_t$, 18.8% for Δc_t, and 86.4% forπ_t

To evaluate the degree of unspanned variation that is generated by the nonlinear structure of the New Keynesian model, the fourth column in Table 7 reports the R^2 values when omitting the quadratic terms in the second-order projection solution and the measurement errors. The R^2 values now increase to 88.9% for $\widehat{l}_t$, 94.6% for $\widehat{w}_t$, 74.1% for Δc_t, and 99.0% for π_t. We do not achieve perfect spanning (i.e., $R^2 = 1$) in this case because consumption habits introduce $\log(c_{t-1}/z_{t-1})$ as an endogenous state variable. The last part of Table 7 shows that an additional principal

https://doi.org/10.1017/S0022109025000079 Published online by Cambridge University Press

component with $K = 6$ allows us to capture the information in this endogenous state and achieve perfect spanning.

Accordingly, the nonlinear structure of the New Keynesian model implies that the first five principal components of bond yields explain a fairly small proportion of the variation in $\widehat{l}_t$ and Δc_t but a much larger proportion of the variation in π_t, which is consistent with U.S. data. For the real wage, the nonlinearities in the model have a somewhat smaller effect, and measurement errors are therefore needed to reduce the R^2 to the level seen in U.S. data. This shows that the proposed model goes a long way in resolving the spanning puzzle. This result may also serve as a more theoretical motivation for imposing the restrictions in Joslin et al. (2014), because these restrictions make their reduced-form DTSM more consistent with an equilibrium model of the type proposed in this article.

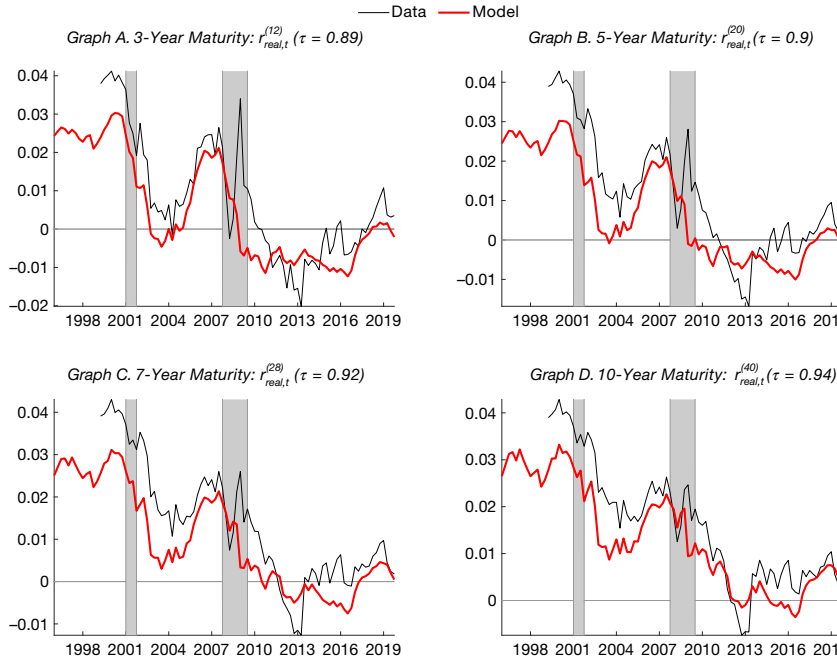
B. Real Bond Yields and Real Term Premia

Figure 5 shows selected real bond yields $r^{(k)}_{real,t}$ from $\mathcal{M}^{M,CS}$, with the corresponding U.S. yields provided by Gürkaynak, Sack, and Wright (2010) from 1999. We see that the model gives a remarkable close fit to historical real yields across all maturities, with correlations between the data and the model-implied series of 0.9 or

FIGURE 5

Real Bond Yields

Figure 5 shows real bond yields in the U.S. as provided by Gürkaynak et al. (2010) and model-implied real yields from $\mathcal{M}^{M,CS}$ evaluated at the estimated states from the CDKF. The value of τ denotes the correlation between the empirical series and the model-implied series. Shaded areas denote NBER recessions.



https://doi.org/10.1017/S0022109025000079 Published online by Cambridge University Press

TABLE 8

Moments Related to Real Bond Yields

Table 8 shows first and second unconditional moments related to real yields in the U.S. from 1999 to 2019 and in the model $\mathcal{M}^{M,CS}$. The model-implied unconditional moments are computed using a simulated series of 100,000 observations. All bond yields are reported in percentages, while all risk premia are in annualized basis points.

	U.S. Data (1999–2019)		Model: $\mathcal{M}^{M,CS}$					
	Real Yields		Real Yields		Real Yerm Premia		Inflation Yisk Premia	
	Mean	Std. Dev.	Mean	Std. Dev.	Mean	Std. Dev.	Mean	Std. Dev.
	1	2	3	4	5	6	7	8
3-year	0.78	1.55	1.13	1.38	7.1	17.9	29.1	17.5
5-year	1.10	1.48	1.33	1.37	26.3	29.4	41.4	27.2
7-year	1.34	1.39	1.54	1.36	47.7	41.0	52.8	35.4
10-year	1.59	1.27	1.89	1.36	82.0	56.8	69.4	44.7

higher. We also note that model-implied real yields are generally slightly below historical yields. This finding is consistent with liquidity risk premia in U.S. real yields, which make these yields higher than implied by a frictionless market (see Abrahams, Adrian, Crump, Moench, and Yu (2016), D'Amico, Kim, and Wei (2018), and Andreasen, Christensen, and Riddell (2021), among others). These liquidity premia are generally estimated to be large in the beginning of the 2000s and around the 2007–2009 Great Recession, which may explain why we at these episodes see somewhat larger differences between our model and U.S. real yields.

Table 8 summarizes key unconditional moments linked to real bond yields, with the model-implied moments computed using a simulated sample of 100,000 observations. We find that the mean and standard deviation of real bond yields in $\mathcal{M}^{M,CS}$ match closely the corresponding empirical moments. Note in particularly that $\mathcal{M}^{M,CS}$ has an upward sloping average real yield curve of $1.89\% - 1.13\% = 0.76\%$, which is very similar to the corresponding empirical slope of $1.59\% - 0.78\% = 0.81\%$. As for nominal bond yields, we compute real term premia as $TP^{(k)}_{real,t} = r^{(k)}_{real,t} - \sum_{i=0}^{k-1} \mathbb{E}_t[r_{real,t+i}]$. The fifth and sixth column in Table 8 show that $\mathcal{M}^{M,CS}$ generates real term premia, which on average are positive and very volatile. For instance, at the 10-year maturity, the real term premium has a mean of 82 basis points and a standard deviation of 57 basis points. Finally, the inflation risk premium is given by the difference between nominal and real term premia (i.e., $TP^{(k)}_t - TP^{(k)}_{real,t}$) and seen to be positive on average and almost as volatile as real term premia.

To summarize, the proposed model provides a close fit to historical real bond yields and their first and second unconditional moments, although none of these moments are included when estimating the New Keynesian model.

C. Equity Returns

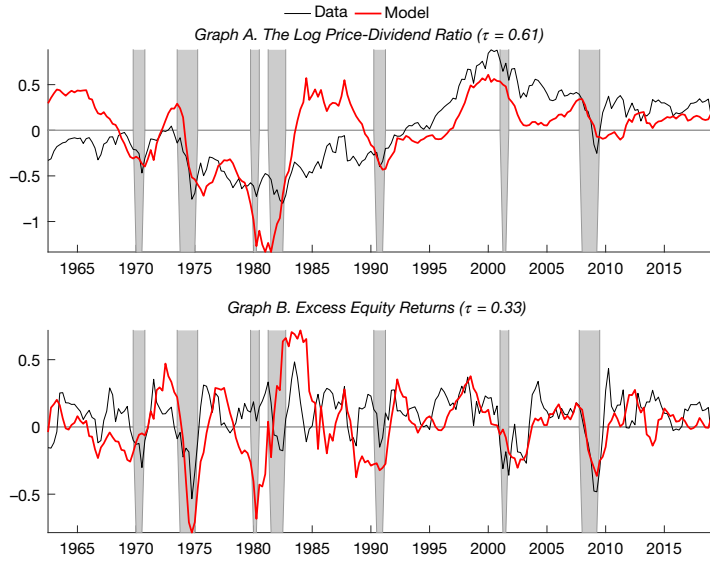
We define the equity return r^{eq}_t as a claim on consumption which constitutes dividends. The real equity price P^{eq}_t is then given by $\mathbb{E}_t\left[M^{real}_{t,t+1} e^{r^{eq}_{t+1}}\right] = 1$, where $e^{r^{eq}_{t+1}} = \left(C_{t+1} + P^{eq}_{t+1}\right)/P^{eq}_t$ and $M^{real}_{t,t+1} = M_{t,t+1}\pi_{t+1}$. Figure 6 shows the log-

https://doi.org/10.1017/S0022109025000079 Published online by Cambridge University Press

FIGURE 6

The Price-Dividend Ratio and Excess Equity Returns

Graph A of Figure 6 shows the log-transformed price-dividend ratio for the U.S. and in $\mathcal{M}^{M,CS}$. Graph B shows the annualized realized excess equity returns in the U.S. and in $\mathcal{M}^{M,CS}$. The model-implied values are evaluated at the estimated states from the CDKF and shaded areas denote NBER recessions.



transformed price-dividend ratio pd_t in the model when evaluated at the estimated states and the corresponding series in the U.S. obtained from the Center for Research in Security and Prices (CRSP) with dividends reinvested in the risk-free rate. The unconditional mean of pd_t in $\mathcal{M}^{M,CS}$ is 4.35 and hence somewhat higher than the sample average of 3.61 for pd_t in our U.S. sample, and we therefore plot the demeaned series in Graph A of Figure 6 to facilitate the comparison. We find that $\mathcal{M}^{M,CS}$ fits the overall evolution in the price-dividend ratio fairly well, particularly during the 1970s and after 1990. The main exception relates to the 1980s, where the model either gives a too low or too high value of pd_t. The correlation between the data and the model-implied series is $\tau = 0.61$. For the considered sample, the model implies a standard deviation of 0.39 for pd_t, which is nearly identical to corresponding sample moment of 0.38 in the U.S.

Graph B of Figure 6 considers the realized excess equity returns $r_t^{ex} \equiv r_t^{eq} - r_{real,t-1}^{(1)}$, where we plot annualized returns. We find that $\mathcal{M}^{M,CS}$ provides a reasonable fit to U.S. excess equity returns from CRSP, although the model gives too volatile returns during the 1980s. As a result, the model implies a standard deviation of 23.9% for excess equity returns, whereas the corresponding sample moment is somewhat lower at 16.4%. The overall correlation between the data and the model-implied series is $\tau = 0.33$.

An important aspect of equity returns relate to their predictability. We explore this issue for excess equity returns, where we regress the accumulated excess returns j periods ahead on the current 10-year yield spread $r_t^{(40)} - r_t^{(4)}$ and the

https://doi.org/10.1017/S0022109025000079 Published online by Cambridge University Press

TABLE 9

Equity Return Predictability

Table 9 shows the regression coefficients and the R^2 when regressing future excess equity returns on the slope of the yield curve and the log-transformed price-dividend ratio. For the empirical data moments, these regressions are computed on quarterly U.S. data from 1961 to 2019. Figures in parentheses for the data moments refer the 95% confidence bands obtained by resampling the regressant and the regressors jointly in blocks of $2 \times j$ using 10,000 samples of the same length $T = 234$ as in the empirical sample. The corresponding model-implied moments for $\mathcal{M}^{M,CS}$ are computed from a simulated sample of 100,000 observations, which are split into samples of length T. The reported results are the average across these $\lfloor 100,000/T \rfloor$ regressions. All variables in the regression are demeaned and scaled to have a unit standard deviation.

	U.S. Data			Model: $\mathcal{M}^{M,CS}$		
	β_j	δ_j	R_j^2	β_j	δ_j	R_j^2
1-year	0.59 (–0.24,1.51)	–0.56 (–1.50,0.33)	0.04 (0.00,0.21)	0.12	−0.37	0.04
2-year	1.40 (0.16,2.67)	–1.69 (–3.28,0.07)	0.14 (0.01,0.40)	0.35	−1.55	0.12
3-year	2.27 (0.74,3.46)	–2.53 (–3.88,–0.22)	0.25 (0.04,0.55)	0.52	−2.57	0.20

price-dividend ratio pd_t following the work of Fama and French (1989). That is, we consider the forecast regression

$$\sum_{i=1}^{j} r_{t+i}^{ex} = \alpha_j + \beta_j \left(r_t^{(40)} - r_t^{(4)} \right) + \delta_j pd_t + v_{t+j}.$$

Table 9 reports the slope coefficients in this regression at selected forecast horizons, with bootstrapped 95% confidence bands provided in parentheses. To ease the comparison with the model, we scale all variables in this regression to have 0 mean and a unit variance. The results show that excess returns in the U.S. are predictable by the 10-year yield spread at the 2- and 3-year horizon and by the price-dividend ratio at the 3-year horizon. We obtain the corresponding model-implied regression loadings in $\mathcal{M}^{M,CS}$ from a simulated sample of 100,000 observations, which we split into samples of the same length $T = 234$ as in the empirical data to account for well-known small-sample biases. The reported results are then the average across these $\lfloor 100,000/T \rfloor$ regressions, where $\lfloor x \rfloor$ denotes the largest integer less than or equal to x. We find that the model generates the desired positive slope coefficients for the yield spread, which increase with the forecast horizon although less strongly when compared to the data. For the price-dividend ratio, we find the desired negative slope coefficients, which closely match the value in the data at all forecast horizons. As a result, the model generates R^2 values of the same magnitude as in empirical data.

To summarize, the proposed New Keynesian model matches several stylized properties of equity prices and equity returns, although these moments are not included when estimating the model.

VII. Conclusion

This article addresses a long-standing ambition in the literature by formulating a New Keynesian model to provide a structural explanation for variation in bond yields and their term premia. The model explains bond yields with a low level of

https://doi.org/10.1017/S0022109025000079 Published online by Cambridge University Press

news in expected inflation and plausible term premia. This implies that the slope of the yield curve predicts future bond yields and that risk-adjusted historical bond yields satisfy the expectations hypothesis. The model goes a long way in explaining the spanning puzzle and matches key moments for real bond yields. Finally, the model also captures the overall evolution of the price-dividend ratio and excess equity returns, and it implies that these returns can be forecasted based on the slope of the yield curve and the price-dividend ratio.

Appendix A. The Projection Approximation

Let $\tilde{c}_t = \frac{c_t}{z_t}$, $\tilde{V}_t = \frac{V_t}{z_t^{1-\chi}}$, $\tilde{w}_t = \frac{w_t}{z_t}$, and $\tilde{y}_t = \frac{y_t}{z_t}$. The equilibrium conditions for a scaled version of the New Keynesian model without trending variables are then easily shown to be given by

EQ 0 $$evf_t = \mathbb{E}_t\left[\left(\widetilde{V}_{t+1}\mu_{z,t+1}^{1-\chi}\right)^{1-\alpha}\right]$$

EQ 1 $$\widetilde{V}_t = u_0 + d_t\left[\frac{1}{1-\chi}\left(\tilde{c}_t - b\tilde{c}_{t-1}\mu_{z,t}^{-1}\right)^{1-\chi} + n_t\varphi_0\frac{(1-l_t)^{1-\frac{1}{\varphi}}}{1-\frac{1}{\varphi}}\right] + \beta evf_t^{\frac{1}{1-\alpha}}$$

EQ 2 $$\tilde{w}_t = \kappa_w\tilde{w}_{ss} + (1-\kappa_w)\left[n_t\varphi_0(1-l_t)^{-\frac{1}{\varphi}}\left(\tilde{c}_t - b\tilde{c}_{t-1}\mu_{z,t}^{-1}\right)^{\chi}\right]$$

EQ 3 $$\mathbb{E}_t[M_{t,t+1}]R_t = 1$$

EQ 4 $$\tilde{w}_t = mc_t(1-\theta)a_t k_{ss}^{\theta} l_t^{-\theta}$$

EQ 5 $$\frac{-1}{\eta mc_t}\left(\xi\left(\frac{\pi_t}{\pi_{ss}}-1\right)\frac{\pi_t}{\pi_{ss}} - (1-\eta) - \mathbb{E}_t\left[\xi M_{t,t+1}\pi_{t+1}\left(\frac{\pi_{t+1}}{\pi_{ss}}-1\right)\frac{\pi_{t+1}}{\pi_{ss}}\frac{\tilde{y}_{t+1}}{\tilde{y}_t}\mu_{z,t+1}\right]\right) = 1$$

EQ 6 $$R_t = R_{ss}\mathbb{E}_t\left[\exp\{\phi_\pi\log\left(\frac{\pi_{t+1}}{\pi_{ss}\pi_{t+1}^*}\right) + \phi_{\Delta c}(\log\left(\frac{\tilde{c}_{t+1}}{\tilde{c}_t}\right) + \log\mu_{z,t+1} - \log\mu_{z,ss})\}\right]$$

EQ 7 $$\tilde{c}_t + \delta k_{ss} = \left(1 - \frac{\xi}{2}\left(\frac{\pi_t}{\pi_{ss}}-1\right)^2\right)\tilde{y}_t$$

EQ 8 $$\tilde{y}_t = a_t k_{ss}^{\theta} l_t^{1-\theta}$$

where evf_t is an auxiliary variable, $\Delta c_{ss} = \log\mu_{z,ss}$, and

$$M_{t,t+1} = \beta\left(\frac{\left[\mathbb{E}_t\left[\left(\widetilde{V}_{t+1}\mu_{z,t+1}^{(1-\chi)}\right)^{1-\alpha}\right]\right]^{\frac{1}{1-\alpha}}}{\widetilde{V}_{t+1}\mu_{z,t+1}^{(1-\chi)}}\right)^{\alpha}\frac{d_{t+1}}{d_t}\frac{\left(\tilde{c}_{t+1} - b\mu_{z,t}^{-1}\tilde{c}_t\right)^{-\chi}}{\left(\tilde{c}_t - b\mu_{z,t-1}^{-1}\tilde{c}_{t-1}\right)^{-\chi}}\mu_{z,t+1}^{-\chi}\frac{1}{\pi_{t+1}}.$$

We first realize that it is sufficient to solve for $\tilde{c}_t$, π_t, and evf_t. The reason is that given these variables, EQ 7 implies $\tilde{y}_t = (\tilde{c}_t + \delta k_{ss})/\left(1 - \frac{\xi}{2}\left(\frac{\pi_t}{\pi_{ss}}-1\right)^2\right)$ and EQ 8 gives $l_t = \left(\frac{\tilde{y}_t}{a_t k_{ss}^{\theta}}\right)^{\frac{1}{1-\theta}}$. From EQ 2 we directly have $\tilde{w}_t$, and $mc_t = \frac{\tilde{w}_t}{(1-\theta)a_t k_{ss}^{\theta} l_t^{-\theta}}$ follows form EQ 4. Finally, EQ 1 gives $\tilde{V}_t$ and EQ 6 gives R_t after evaluating the conditional

https://doi.org/10.1017/S0022109025000079 Published online by Cambridge University Press

expectation. Accordingly, the model can be condensly expressed by the three Euler-equations in EQ 0, EQ 3, and EQ 5. We evaluate conditional expectations using the monomial (non-product) integration rule of Judd, Maliar, and Maliar (2011) to obtain the Euler-equation errors $\mathbf{r}(\mathbf{x}_i) = \left[r^{EQ0}(\mathbf{x}_i) \;\; r^{EQ3}(\mathbf{x}_i) \;\; r^{EQ5}(\mathbf{x}_i) \right]'$ for each point $\mathbf{x}_i$ in the grid $\mathcal{X}$. The Euler-errors for EQ 3 and EQ 5 are expressed in unit-free terms. A similar scaling is not adopted for EQ 0 because preliminary results showed that the level of evf_t then became badly identified and most often implausible large in the approximation. As for the grid, we express $\mathbf{x}_i$ in deviation from the deterministic steady state. The work of Judd, Maliar, Maliar, and Valero (2014) is used to construct a multidimensional Smolyak grid of order 2 for the hypercube $\prod_{i=1}^{n_x} [\mu_i - 1.5\sigma_i, \mu_i + 1.5\sigma_i]$, where μ_i and σ_i are the unconditional mean and standard deviation, respectively, of the i state variable. For the five shocks, the model is expressed such that $\mu_i = 0$ and we easily obtain σ_i from equation (10). For the last element $\tilde{c}_{t-1}$ in the state vector, we use a second-order perturbation approximation and the results in Andreasen et al. (2018) to compute its unconditional mean μ_i in deviation from the deterministic steady state, while we use a first-order perturbation approximation to get σ_i. Applying a standard log-transformation to all variables, all loadings related to the three variables in $\mathbf{y}_t^a$ are then obtained by nonlinearly minimizing $\sum_{i=1}^{N} \frac{\mathbf{r}(\mathbf{x}_i)'\mathbf{r}(\mathbf{x}_i)}{\left(1+\mathbf{x}_i'\mathbf{x}_i\right)^2}$, where $N = 85$ is the number of grid points for our configuration. The scaling $1/\left(1+\mathbf{x}_i'\mathbf{x}_i\right)^2$ is introduced to assign less weight to points far from the steady state to ensure that the approximation is very accurate close to the steady state.

Given this solution for $\mathbf{y}_t^a$, we can compute the additional macro variables in $\mathbf{y}^b(\mathbf{x}_i)$ for all grid points and run the OLS regression

$$\mathbf{y}^b(\mathbf{x}_i) = \mathbf{g}_0^b + \mathbf{g}_{\mathbf{x}}^b \mathbf{x}_i + \mathbf{g}_{\mathbf{xx}}^b vech\left(\mathbf{x}_i \mathbf{x}_i'\right) + \mathbf{u}_i^b$$

to instantaneously get the loadings $\mathbf{g}_0^b$, $\mathbf{g}_{\mathbf{x}}^b$, and $\mathbf{g}_{\mathbf{xx}}^b$ with dimensions 2×1, $2 \times n_x$, and $2 \times n_x(n_x+1)/2$, respectively.

To obtain all bond prices, for $k = 1$ we can compute $B_t^{(1)}(\mathbf{x}_i) = \mathbb{E}_t[M_{t,t+1}(\mathbf{x}_i)]$ for all grid points using the solution for $\mathbf{y}_t^a$ and numerical integration. We then compute $b_t^{(1)}(\mathbf{x}_i) = \log B_t^{(1)}(\mathbf{x}_i)$ and regress $b_t^{(1)}(\mathbf{x}_i)$ on a constant, $\mathbf{x}_i$, and $vech\left(\mathbf{x}_i \mathbf{x}_i'\right)$ to get the loadings for $b_t^{(1)}$. For $k = 2$, we use the these loadings to compute $B_t^{(2)} = \mathbb{E}_t\left[M_{t,t+1}(\mathbf{x}_i) B_{t+1}^{(1)}(\mathbf{x}_i)\right]$ in a similar manner. Then we compute $b_t^{(2)}(\mathbf{x}_i) = \log B_t^{(2)}(\mathbf{x}_i)$ and regress $b_t^{(2)}(\mathbf{x}_i)$ on a constant, $\mathbf{x}_i$, and $vech\left(\mathbf{x}_i \mathbf{x}_i'\right)$ to get the loadings for $b_t^{(2)}$. We continue in this way until we have the entire 10-year yield curve.

Finally, for expected short rates $r_{t|k}^e \equiv \mathbb{E}_t[r_{t+k}]$, we first compute $r_{t|1}^e(\mathbf{x}_i) = \mathbb{E}_t\left[-b_{t+1}^{(1)}(\mathbf{x}_i)\right]$ for all grid points using the solution for $b_t^{(1)}$ and numerical integration. Then we regress $r_{t|1}^e(\mathbf{x}_i)$ on a constant, $\mathbf{x}_i$, and $vech\left(\mathbf{x}_i \mathbf{x}_i'\right)$ to get the loadings for $r_{t|1}^e$. We then use these loadings and numerical integration to compute $r_{t|2}^e(\mathbf{x}_i) = \mathbb{E}_t\left[r_{t+1|1}^e(\mathbf{x}_i)\right]$ for all grid points, and the required loadings are obtained by regressing $r_{t|2}^e(\mathbf{x}_i)$ on a constant, $\mathbf{x}_i$, and $vech\left(\mathbf{x}_i \mathbf{x}_i'\right)$. We continue in this way until we have all the desired short rate expectations needed to compute term premia at the desired horizon.

https://doi.org/10.1017/S0022109025000079 Published online by Cambridge University Press

Supplementary Material

To view supplementary material for this article, please visit http://doi.org/10.1017/S0022109025000079.

Funding Statement

I acknowledge funding from the Independent Research Fund Denmark, project number 7024-00020B and support from the Danish Finance Institute (DFI).

References

Abrahams, M.; T. Adrian; R. K. Crump; E. Moench; and R. Yu. "Decomposing Real and Nominal Yield Curves." *Journal of Monetary Economics*, 84 (2016), 182–200.

Adrian, T.; R. K. Crump; and E. Moench. "Pricing the Term Structure with Linear Regressions." *Journal of Financial Economics*, 110 (2013), 110–138.

Albuquerque, R.; M. Eichenbaum; V. X. Luo; and S. Rebelo. "Valuation Risk and Asset Pricing." *Journal of Finance*, 71 (2016), 2861–2904.

Altig, D.; L. J. Christiano; M. Eichenbaum; and J. Linde. "Firm-Specific Capital, Nominal Rigidities and the Business Cycle." *Review of Economic Dynamics*, 14 (2011), 225–247.

Andreasen, M. M. "How to Maximize The Likelihood Function for a DSGE Model." *Computational Economics*, 35 (2010), 127–154.

Andreasen, M. M. "On the Effects of Rare Disasters and Uncertainty Shocks for Risk Premia in Non-Linear DSGE Models." *Review of Economic Dynamics*, 15 (2012), 295–316.

Andreasen, M. M. "Non-Linear DSGE Models and the Central Difference Kalman Filter." *Journal of Applied Econometrics*, 28 (2013), 929–955.

Andreasen, M. M.; J. H. E. Christensen; and S. Riddell. "The TIPS Liquidity Premium." *Review of Finance*, 25 (2021), 1639–1675.

Andreasen, M. M.; J. Fernandez-Villaverde; and J. F. Rubio-Ramirez. "The Pruned State Space System for Non-Linear DSGE Models: Theory and Empirical Applications to Estimation." *Review of Economic Studies*, 85 (2018), 1–49.

Andreasen, M. M., and K. Jørgensen. "The Importance of Timing Attitudes in Consumption-Based Asset Pricing Models." *Journal of Monetary Economics*, 111 (2020), 95–117.

Aruoba, S. B.; J. Fernandez-Villaverde; and J. F. Rubio-Ramirez. "Comparing Solution Methods for Dynamic Equilibrium Economies." *Journal of Economic Dynamics and Control*, 30 (2006), 2477–2508.

Bansal, R., and A. Yaron. "Risks for the Long Run: A Potential Resolution of Asset Pricing Puzzles." *Journal of Finance*, 59 (2004), 1481–1509.

Bauer, M. D., and G. D. Rudebusch. "Resolving the Spanning Puzzle in Macro-Finance Term Structure Models." *Review of Finance*, 21 (2017), 511–553.

Bekaert, G.; S. Cho; and A. Moreno. "New Keynesian Macroeconomics and the Term Structure." *Journal of Money, Credit and Banking*, 42 (2010), 33–62.

Binsbergen, J. H. V.; J. Fernandez-Villaverde; R. S. Koijen; and J. Rubio-Ramirez. "The Term Structure of Interest Rates in a DSGE Model with Recursive Preferences." *Journal of Monetary Economics*, 59 (2012), 634–648.

Blanchard, O., and J. Gali. "Real Wage Rigidities and the New Keynesian Model." *Journal of Money, Credit and Banking*, 39 (2005), 35–65.

Bretscher, L.; A. Hsu; and A. Tamoni. "Fiscal Policy Driven Bond Risk Premia." *Journal of Financial Economics*, 138 (2020), 53–73.

Caldara, D.; J. Fernandez-Villaverde; J. F. Rubio-Ramirez; and W. Yao. "Computing DSGE Models with Recursive Preferences and Stochastic Volatility." *Review of Economic Dynamics*, 15 (2012), 188–206.

Campbell, J. Y., and R. J. Shiller. "Yield Spread and Interest Rate Movements: A Bird's Eye View." *Review of Economic Studies*, 58 (1991), 495–514.

Chernozhukov, V., and H. Hong. "An MCMC Approach to Classical Estimation." *Journal of Econometrics*, 115 (2003), 293–346.

https://doi.org/10.1017/S0022109025000079 Published online by Cambridge University Press

Christiano, L. J.; M. Trabandt; and K. Walentin. "Introducing Financial Frictions and Unemployment into a Small Open Economy Model." *Journal of Economic Dynamic and Control*, 35 (2011), 1999–2041.
Cochrane, J. H. "Financial Markets and the Real Economy." In *Handbook of the Equity Risk Premium*, R. Mehra, ed. Oxford, UK: Elsevier (2007), 237–330.
Dai, Q., and K. J. Singleton. "Expectation Puzzles, Time-Varying Risk Premia and Affine Models of the Term Structure." *Journal of Financial Economics*, 63 (2002), 415–441.
D'Amico, S.; D. H. Kim; and M. Wei. "Tips from TIPS: The Informational Content of Treasury Inflation-Proctected Security Prices." *Journal of Financial and Quantitative Analysis*, 53 (2018), 395–436.
Dew-Becker, I. "Bond Pricing with a Time-Varying Price of Risk in an Estimated Medium-Scale Bayesian DSGE Model." *Journal of Money Credit and Banking*, 46 (2014), 837–888.
Duffee, G. R. "Expected Inflation and Other Determinants of Treasury Yields." *The Journal of Finance*, 73 (2018), 2139–2180.
Epstein, L. G.; E. Farhi; and T. Strzalecki. "How Much Would You Pay to Resolve Long-Run Risk?" *American Economic Review*, 104 (2014), 2680–2697.
Epstein, L. G., and S. E. Zin. "Substitution, Risk Aversion, and the Temporal Behavior of Consumption and Asset Returns: A Theoretical Framework." *Econometrica*, 57 (1989), 937–969.
Fama, E. F., and K. R. French. "Business Conditions and Expected Returns on Stocks and Bonds." *Journal of Financial Economics*, 25 (1989), 23–49.
Fernández-Villaverde, J., and J. F. Rubio-Ramírez. "Estimating Macroeconomic Models: A Likelihood Approach." *Review of Economic Studies*, 74 (2007), 1–46.
Fisher, J. D. M. "The Dynamic Effects of Neutral and Investments-Specific Technology Shocks." *Journal of Political Economy*, 114, no. 3 (2006), 413–451.
Gomez-Cram, R., and A. Yaron. "How Important are Inflation Expectations for the Nominal Yield Curve?" *Review of Financial Studies*, 34 (2021), 985–1045.
Graeve, F. D.; M. Emiris; and R. Wouters. "A Structural Decomposition of the US Yield Curve." *Journal of Monetary Economics*, 56 (2009), 545–559.
Gürkaynak, R.; B. Sack; and J. Wright. "The U.S. Treasury Yield Curve: 1961 to the Present." *Journal of Monetary Economics*, 54 (2007), 2291–2304.
Gürkaynak, R. S.; B. Sack; and J. H. Wright. "The TIPS Yield Curve and Inflation Compensation." *American Economic Journal: Macroeconomics*, 2 (2010), 70–92.
Hall, R. E. "Intertemporal Substitution in Consumption." *Journal of Political Economy*, 96 (1988), 339–357.
Hamilton, J. D. "Why You Should Never Use the Hodrick-Prescott Filter." *Review of Economics and Statistics*, 100 (2018), 831–843.
Hansen, L. P. "Large Sample Properties of Generalized Method of Moments Estimators." *Econometrica*, 50 (1982), 1029–1054.
Hordahl, P.; O. Tristani; and D. Vestin. "The Yield Curve and Macroeconomic Dynamics." *The Economic Journal*, 118 (2008), 1937–1970.
Joslin, S.; M. A. Priebsch; and K. J. Singleton. "Risk Premiums in Dynamic Term Structure Models with Unspanned Macro Risks." *The Journal of Finance*, 69 (2014), 1197–1233.
Judd, K. L. "Projection Methods for Solving Aggregate Growth Models." *Journal of Economic Theory*, 58 (1992), 410–452.
Judd, K. L.; L. Maliar; and S. Maliar. "Numerically Stable and Accurate Stochastic Simulation Approaches for Solving Dynamic Economic Models." *Quantitative Economics*, 2 (2011), 173–210.
Judd, K. L.; L. Maliar; S. Maliar; and R. Valero. "Smolyak Method for Solving Dynamic Economic Models: Lagrange Interpolation, Anisotropic Grid and Adaptive Domain." *Journal of Economic Dynamics and Control*, 44 (2014), 92–123.
Keane, M. P. "Labor Supply and Taxes: A Survey." *Journal of Economic Literature*, 49 (2011), 961–1075.
Kreps, D. M., and E. L. Porteus. "Temporal Resolution of Uncertainty and Dynamic Choice Theory." *Econometrica*, 46 (1978), 185–200.
Kung, H. "Macroeconomic Linkages between Monetary Policy and the Term Structure of Interest Rates." *Journal of Financial Economics*, 115 (2015), 42–57.
Lagerborg, A.; E. Pappa; and M. O. Ravn. "Sentimantal Business Cycles." *Review of Economic Studies*, 90 (2023), 1358–1393.
Levintal, O. "Fifth-Order Perturbation Solution to DSGE Models." *Journal of Economics Dynamic and Control*, 80 (2017), 1–16.
Meyer-Gohde, A., and M. Kliem. "(Un)expected Monetary Policy Shocks and Term Premia." *Journal of Applied Econometrics*, 37 (2022), 477–499.

https://doi.org/10.1017/S0022109025000079 Published online by Cambridge University Press

Nakata, T., and H. Tanaka. "Equilibrium Yield Curves and the Interest Rate Lower Bound." Finance and Economic Discussion Series, Federal Reserve Board, Washington D.C., (2016).
Norgaard, M.; N. K. Poulsen; and O. Ravn. "Advances in Derivative-Free State Estimation for Nonlinear Systems." *Automatica*, 36 (2000), 1627–1638.
Piazzesi, M., and M. Schneider. "Equilibrium Yield Curves." In *NBER Macroeconomics Annual 2006*, Vol. 21, D. Acemoglu, K. Rogoff, and M. Woodford, eds. Cambridge, MA: MIT Press (2007), 389–442.
Rotemberg, J. J. "Monopolistic Price Adjustment and Aggregate Output." *Review of Economic Studies*, 49 (1982), 517–531.
Rudebusch, G. D., and E. T. Swanson. "Examining the Bond Premium Puzzle with a DSGE Model." *Journal of Monetary Economics*, 55 (2008), 111–126.
Rudebusch, G. D., and E. T. Swanson. "The Bond Premium in a DSGE Model with Long-Run Real and Nominal Risks." *American Economic Journal: Macroeconomics*, 4 (2012), 1–43.
Smets, F., and R. Wouters. "Shocks and Frictions in US Business Cycles: A Bayesian DSGE Approach." *American Economic Review*, 97 (2007), 586–606.
Swanson, E. T. "Risk Aversion, Risk Premia, and the Labor Margin with Generalized Recursive Preferences." *Review of Economic Dynamics*, 28 (2018), 290–321.
Weil, P. "Nonexpected Utility in Macroeconomics." *Quarterly Journal of Economics*, 105 (1990), 29–42.
Yogo, M. "Estimating the Elasticity of Intertemporal Substitution When Instruments Are Weak." *Review of Economics and Statistics*, 86 (2004), 797–810.

https://doi.org/10.1017/S0022109025000079 Published online by Cambridge University Press